AD-A219 035

REPORT DOCUMENTATION PAGE

1a. REPORT SECURITY CLASSIFICATION: Unclassified	1b. RESTRICTIVE MARKINGS
2a. SECURITY CLASSIFICATION AUTHORITY	3. DISTRIBUTION / AVAILABILITY OF REPORT: Approved for public release; distribution unlimited.
2b. DECLASSIFICATION / DOWNGRADING SCHEDULE	
4. PERFORMING ORGANIZATION REPORT NUMBER(S)	5. MONITORING ORGANIZATION REPORT NUMBER(S): ARO 25416.1-EG-SDI
6a. NAME OF PERFORMING ORGANIZATION: North Carolina State University; 6b. OFFICE SYMBOL (If applicable)	7a. NAME OF MONITORING ORGANIZATION: U. S. Army Research Office
6c. ADDRESS (City, State, and ZIP Code): Department of Nuclear Engineering, Box 7909 , Raleigh, NC 27695-7909	7b. ADDRESS (City, State, and ZIP Code): P. O. Box 12211, Research Triangle Park, NC 27709-2211
8a. NAME OF FUNDING / SPONSORING ORGANIZATION: U. S. Army Research Office; 8b. OFFICE SYMBOL (If applicable)	9. PROCUREMENT INSTRUMENT IDENTIFICATION NUMBER: DAAL03-87-K-0103
8c. ADDRESS (City, State, and ZIP Code): P. O. Box 12211, Research Triangle Park, NC 27709-2211	10. SOURCE OF FUNDING NUMBERS: PROGRAM ELEMENT NO. / PROJECT NO. / TASK NO. / WORK UNIT ACCESSION NO

11. TITLE (Include Security Classification)
Control of Surface Melting and Ablation in Electromagnetic Launchers via the Magnetic Vapor Shielding Mechanism

12. PERSONAL AUTHOR(S)
Dr. John G. Gilligan

13a. TYPE OF REPORT	13b. TIME COVERED	14. DATE OF REPORT (Year, Month, Day)	15. PAGE COUNT
Final	FROM 7/87 TO 12/89	December 31, 1989	43

16. SUPPLEMENTARY NOTATION
The view, opinions and/or findings contained in this report are those of the author(s) and should not be construed as an official Department of the Army position, policy, or decision, unless so designated by other documentation.

17. COSATI CODES		
FIELD	GROUP	SUB-GROUP

18. SUBJECT TERMS (Continue on reverse if necessary and identify by block number)
Surface melting, surface ablation, vapor shield, magnetic vapor shield, electromagnetic launchers, high heat flux

19. ABSTRACT (Continue on reverse if necessary and identify by block number)

The project has been successful in designing, constructing and operating (over 200 shots) the proof-of-principle experiment SIRENS to simulate the exposure of material surfaces to high heat fluxes under EM and ET launchers conditions. The vapor shield concept has been experimentally verified and the energy transmission factor through the vapor shield varies from 20% to 5% as the heat flux increases. Different material surfaces were tested which revealed that the metallic surfaces have strong axial erosion dependence, while insulators have equal ablation along the axial direction. The heat flux is found to be approximately constant along the barrel axis, with an average plasma velocity of 10 - 12 km/s. Multiple exposure of material surfaces showed that about 190 exposures (at 1 kJ input energy) causes an increase of 20% in the inner bore diameter. There is initial indications of a reduction in ablation with applied magnetic fields above 5 Tesla, for insulator materials (Lexan).

20. DISTRIBUTION / AVAILABILITY OF ABSTRACT	21. ABSTRACT SECURITY CLASSIFICATION
☐ UNCLASSIFIED/UNLIMITED ☐ SAME AS RPT. ☐ DTIC USERS	Unclassified
22a NAME OF RESPONSIBLE INDIVIDUAL	22b. TELEPHONE (Include Area Code) / 22c. OFFICE SYMBOL

DD FORM 1473, 84 MAR — 83 APR edition may be used until exhausted. All other editions are obsolete.

SECURITY CLASSIFICATION OF THIS PAGE
UNCLASSIFIED

CONTROL OF SURFACE MELTING AND ABLATION IN ELECTROMAGNETIC LAUNCHERS VIA THE MAGNETIC VAPOR SHIELDING MECHANISM

FINAL REPORT

By

J. Gilligan, M. Bourham, O. Hankins, O. Auciello, B. Wehring

DECEMBER 31, 1989

U. S. ARMY RESEARCH OFFICE

(DAAL03-87-K-0103)

SUPPORTING THE STRATEGIC DEFENCE INITIATIVE / IST

North Carolina State University
Department of Nuclear Engineering
Raleigh, North Carolina 27695-7909

**APPROVED FOR PUBLIC RELEASE;
DISTRIBUTION UNLIMITTED.**

TABLE OF CONTENTS

ABSTRACT

The project has been successful in designing, constructing and operating (over 200 shots) the proof-of-principle experiment SIRENS to simulate the exposure of material surfaces to high heat fluxes under EM and ET launchers conditions. The vapor shield concept has been experimentally verified and the energy transmission factor through the vapor shield varies from 20% to 5% as the heat flux increases. Different material surfaces were tested which revealed that the metallic surfaces have strong axial erosion dependence. while insulators have equal ablation along the axial direction. The heat flux is found to be approximately constant along the barrel axis, with an average plasma velocity of 10 - 12 km/s. Multiple exposure of material surfaces showed that about 190 exposures (at 1 kJ input energy) cause an increase of 20% in the inner bore diameter. There is initial indications of a reduction in ablation with applied magnetic fields above 5 Tesla, for insulator materials (Lexan).

FINAL REPORT

CONTROL OF SURFACE MELTING AND ABLATION IN ELECTROMAGNETIC LAUNCHERS VIA THE MAGNETIC VAPOR SHIELDING MECHANISM

Contract Period (July 15, 1987 - December 31, 1989)

J. Gilligan, M. Bourham, O. Hankins, O, Auciello, B. Wehring

Department of Nuclear Engineering

North Carolina State University

INTRODUCTION

This final report summarizes experimental work accomplished on our project entitled "Control of Surface Melting and Ablation in Electromagnetic Launchers Via the Magnetic Vapor Shield Mechanism" (DAAL03-87-K-0103). The time period of the contract ran from July 1987 through December of 1989 with total support of approximately $300,000. It is likely that funding of this project (through the SDI) will continue at a level of $612,000 for three years. A companion project for the theory and numerical modeling has been funded by the ARO at a level of approximately $151,000 from January 1986 through September of 1989.

OVERVIEW

Ablation and melting of surfaces in Electromagnetic and Electrothermal launchers due to plasma-material interaction are of fundamental concern to research areas supported by the Department of Defense. The plasmas in these devices can expose surfaces to heat fluxes greater than 10^{10} W/m^2 for a duration of 1 - 100 μs. The goal of our research is to experimentally control and analyze the surface erosion of the EM and ET launchers components via the magnetic vapor shielding concept [1-2]. The basic vapor shield mechanism has been observed by our group as well as by others [2-3]. Selected material samples are exposed to a plasma source which produces high heat fluxes equivalent to those produced in railguns, gun barrels, etc. The ablation of internal insulators and electrodes exposed to the radiation from the accelerating plasma in railguns is of special concern to the ARO (SDI/IST). A proof-of-principle device SIRENS (Surface Interaction Research Experiment at North Carolina State University) was proposed to study the phenomena occurring during the interaction of a high heat flux with material surfaces under the influence of a high-intensity parallel magnetic field [4]. SIRENS has been constructed, tested for operation, and performed over 200 fully diagnosed shots over the contract period. It uses a 300 μF capacitor is charged up to 10 kV (15 kJ stored energy), and is discharged via a spark-gap switch providing a current up to 100 kA through the plasma-source electrode. The plasma is formed by the ablation of the hollow cylindrical insulator. The plasma pressure forces the plasma out through the material sample section. Different material surfaces (conductors and insulators) were tested with and without the magnetic field. Multiple exposure of the same sample was also performed. Preliminary measurements showed that a threshold value of the magnetic field is required for the onset of the magnetic vapor shield effect.

GOALS OF THE PROJECT

. To understand and control the basic energy transport phenomena in the vapor shield at a material surface under high heat loading.

. To explore the effect of a strong magnetic field in decreasing the surface erosion under high heat loading.

PRINCIPAL PROJECT ACCOMPLISHMENTS (1987-1989)

. Design, construct and functional testing of the SIRENS electrothermal launcher was accomplished.

. Experimental verification of the vapor shield effect was confirmed. Energy transmission factor through the vapor shield is on the order of 10% .

. Conditioning effects of single material samples exposed to multiple shots were noted, which will be important in operation of railguns.

. Erosion of different materials was explored. Aluminum and copper are found to melt but Lexan primarily ablates.

. Axial dependence of discharge erosion was measured for different materials.

. The spectra of observed plasma light emission indicated the presence of electrode and sample materials.

. SEM, EDXA and Auger analyses demonstrate the redeposition of electrode materials at different locations.

. Magnetic fields decreased surface erosion by about 20% for fields of 5 Tesla. Higher fields will be explored in our next study phase.

. Twelve conference presentations, eight refereed publications and one invited talk have been given on the vapor shield project. Dr. J. Gilligan was awarded the NCSU College of Engineering Alcoa Research Prize for work on the project over the past three years.

. One Master thesis and one Ph.D. thesis have been produced. Three current graduate students are partially or fully supported by the project.

M.S., 1989, J. Stock: Surface Erosion of Materials Subjected to High Heat Fluxes from Plasmas (O. Auciello, advisor).

Ph.D.,1990, D. Hahn: Energy Transport Through a Plasma Boundary Layer (J. Gilligan, advisor).

Expected in 1990:

M.S., S. Tallavarjula

M.S., R. Rustad

Ph.D., R. Mohanti

PROJECT RESULTS AND DISCUSSION

The concept of vapor shielding was noted in related applications [5-7] with few detailed calculations and crude estimates for the total energy fraction transmitted through the vapor shield in the range of 50% [6]. Such results did not agree with experimental measurements for laser light incident on surfaces which showed lower values of 10 - 20% [7]. Under the typical conditions experienced in railguns (heat flux, duration etc.) SIRENS was designed to produce high density low temperature plasmas so that the vapor shield would be optically thick enough to absorb the incident radiation.

SIRENS consists of a plasma discharge source, a magnet to produce a parallel high-intensity magnetic field, a high vacuum system, and appropriate diagnostics [4]. Fig.1 shows a schematic drawing of SIRENS; a 300 μF Maxwell capacitor is charged (up to 10 kV) and subsequently discharged to the plasma gun electrode by releasing the stored energy (up to 15 kJ). The discharge is controlled by a spark-gap switch such that a discharge current of up to 100 kA will flow through the gun electrode. The plasma is formed and transported through an annular region to reach the material sample which is placed inside a concentric barrel. A high intensity (up to 20 T) magnetic field parallel to the tube sample axis provides the necessary field for altering the energy transport in the ablated plasma. The magnetic field is produced by a copper coil energized by a current up to 2000 A and the coil is cooled to liquid nitrogen temperature. Fig. 2 shows the plasma source and the sample test section, while fig. 3 shows a cross-sectional elevation of the assembled parts. Fig. 4 shows the peak discharge current for different values of input energy. Discharge current, potential, I -dot and plasma current were measured for each shot using Rogowski

coils and high voltage probe via a Le Croy 8 - channel digitizer. Fig. 5 shows SIRENS efficiency as a function of the stored energy, which indicates that SIRENS reaches 90% efficiency at 3 kJ initial stored energy, and increases to 97% at energies between 4 to 5 kJ, which is indicative of a very efficient energy dump to the plasma in the form of Ohmic heating. The plasma bulk velocity was measured using B-dot coils, Rogowski coils and phototransistors, which indicate that the plasma bulk velocity is 10 - 12 km/s.

VAPOR SHIELD INSIDE THE SOURCE:

In order to study the ablation of the source insulator, a set of Lexan disposable sleeves (which could be situated inside the main Lexan insulator) were fabricated to make easy the weight loss measurements before and after the plasma exposure, and to keep the main insulator from being damaged. Both the main insulator and the disposable sleeves were fabricated from Lexan (polycarbonate), and each sleeve was subjected to a single exposure at a preset input energy. Ablation depth was calculated by taking the weight loss of the sleeve, and using an algorithm to transfer the weight loss into ablation depth (the algorithm includes the dimensions and density of the used sleeve). Fig. 6 shows the ablation depth of the source insulator at different input energies, the experimental results are shown by the "diamonds" while the theoretical results are shown by the solid line curves at different values of "f" which represents the fraction of the energy transport through the vapor shield [8-9]. The theoretical results are obtained from the ZEUS code (0-D time dependent computer code which simulates the plasma condition in the electrothermal gun breech region)[10]. The results show that the energy transmission factor varies between 20% to 5% as the energy input increases, which is indicative of more vapor shielding at higher energies. Typical Lexan ablation depth turn out to be 10 - 14 μm per kJ.

EROSION OF MATERIALS:

Materials under test were arranged either in a complete tubular form of 5 inch length, or in splitted tubular form of 0.5 inch length. The 10 splitted samples were used together to form one complete sample, in order to measure the axial erosion distribution. Samples, complete or splitted, were exposed to the plasma driven from the source at different energies and the erosion depth was calculated. Each sample was exposed once per each energy and some of the shots were repeated to confirm the obtained results and check reproducibility. Lexan, Aluminum, Copper, coarse and fine grain graphite were tested.

LEXAN

Fig. 7 shows the axial dependence of Lexan ablation at energies between 1 and 5 kJ which shows little axial variation, as the plasma cools off during the transport down the barrel. It is also obvious that the ablation depth starts to saturate at higher energies (4 - 5 kJ) indicating the formation of more vapor. Fig. 8 shows a 3-D graph for the ablation depth at different input energies along the axial distance, which shows the saturated ablation at 4-5 kJ, while the ablation along the axial distance is approximately equal. Normalization of the ablation depth showed that the amount of ablation per unit energy decreases as input energy increases, as shown in fig. 9, which is also supported by the optical measurements given by fig. 10. It is obvious that the magnitude of the emission increased with the increased input energy from 1 to 4 kJ and then decreased for 5 kJ. This suggests that the onset of the vapor shielding may be shielding the fiber optic from light. The SEM shows the surface of the exposed Lexan which is indicative of ablation, as shown in fig. 11 .

ALUMINUM

Splitted aluminum samples were exposed to plasma and weighed separately and the erosion depth for each section was calculated. Fig. 12 shows the erosion depth of aluminum along the axial distance, at energies from 1 to 5 kJ. At 1 kJ, the first three sections were eroded with the amount of erosion decreasing with distance from the source. The successive sections had a net weight gain indicating a redeposition. With increasing energy input, the amount of erosion per section increased and sections showing a net weight loss were farther away from the source. This is obvious from the 3-D graph of fig. 13 which clearly indicates the strong axial dependence at all values of input energy. Fig. 14 shows the SEM photograph of the exposed aluminum which indicates melting, resolidification and redeposition. EDXA analysis supports the melting and resolidification of the surfaces, and fig. 15 shows a comparison between a clean aluminum sample and a plasma exposed sample which clearly shows the appearance of nickel, copper, zinc and tungsten. The Auger microprobe analysis supports such results as shown in fig. 16 . Optical emission measurements indicated lines that were characteristic of the tungsten alloy electrodes, the brass connector, the Lexan insulator, and the argon filling gas. A few of the more prominent emission lines are indicated in fig. 17 .

COPPER

A series of experiments was run using copper samples that had been split into 10 identical sub-samples. The experiment showed a strong axial erosion dependence with faster rate of decrease along the axis compared to aluminum. Some sub-samples showed an increase in the weight which indicates a redeposition and a quick cooling off of the plasma as shown in Fig. 18 and the 3-D graph of fig. 19. SEM, EDXA and Auger data analysis indicate the

melting and resolidification of the surfaces and the erosion of the electrodes material as shown in fig. 20, 21 and 22 .

The self-segregating copper-lithium alloy (where a lithium layer naturally replenishes itself on the surface) showed that the erosion is only slightly less than pure copper. Comparison with pure copper erosion at the same energy is shown in fig. 23 .

GRAPHITE

Two different grades of graphite [11] were tested, high density graphite of maximum grain size 800 μm (grade 6222) and molded dense electrographite of maximum grain size 40 μm (grade 2020). Grade 6222 showed strong axial redeposition for lower energy inputs up to 3 kJ, slight ablation at 4 kJ, and a tendency towards less ablation at energies above 4 kJ. Grade 2020 showed axial ablation dependence for the sub-samples close to the source followed by approximate equal ablation for the subsequent sub-samples, with a decreasing ablation depth for energies above 4 kJ. Such decrease in the ablation depth could be due to the vapor shield as more vaporization is expected at higher energy inputs. Fig. 24 shows the ablation axial dependence of the grade 2020 graphite.

COMPARISON BETWEEN DIFFERENT TESTED MATERIALS

In order to compare the erosion of the tested material surfaces, the erosion depth of the individual sub-samples is averaged over the full length which represents the total barrel length, for the input energies from 1 to 5 kJ. Fig. 25 shows the erosion depth of aluminum, copper, Lexan, graphite 6222 and graphite 2020. It is clear from the figure that the metallic surfaces (aluminum and copper) show an increasing erosion depth with the

increase of the input energy. Lexan shows an increasing ablation depth with the increase in the energy input, with tendency to saturate at energies above 4 kJ. High density graphite (grade 6222) shows resistance to ablation at lower energies (1 - 3 kJ) and net deposition was observed. At 4 kJ input energy, it starts to ablate at considerably low rate with tendency towards a decreasing or saturated ablation at 5 kJ. The molded dense electrographite ablates at all values of energy input with an increasing rate of ablation up to 4 kJ input energy, and the rate decreases with the increase in the energy input above 4 kJ. The behavior of Lexan and graphite is indicative of the formation of vapor shield, where a fraction of the incoming energy will be absorbed through the vapor layer. In order to get a better view of the erosion and ablation of the above materials, fig. 26 represents the normalized values per unit energy input (per kJ). Such normalization yields a better view of the erosion and ablation processes in view of the vapor shield concept. It is obvious from the graph that the erosion depth per unit energy input (1 kJ) decreases with the increase in energy input for Lexan which is indicative of the vapor shield at all values of input energy. The high density graphite and molded dense electrographite have an onset for the vapor shield at 4 kJ, and the ablation rate decreases with the energy increase. Metallic surfaces at lower energies may not acquire the vapor shield process because of melting rather than vaporization, while at higher energies the vaporization may be the dominant factor and consequently the development of vapor shield may take place. Above 4 kJ of input energy, the metallic surfaces (aluminum and copper) show a saturated or decreasing rate of erosion which may be indicative of the absorption of the incoming energy through the vapor shield.

SPECIALLY ARRANGED SAMPLES

A self-segragated copper-lithium alloy sample sections together with Lexan sample sections were arranged to form a complete one test sample. The first 5 sections were from Cu-Li followed by 5 sections of Lexan, and then exposed to a 3kJ input energy. Comparison between Lexan ablation of the special sample with that of a fully-splitted one at the same input energy showed that the ablation depth is approximately 50% less as shown in fig. 27 . Repeating the same procedure using graphite 6222 instead of the Cu-Li at 5 kJ input energy showed that the ablation of Lexan is also about 50% less as shown in fig. 28 . Assuming that the heat flux down the barrel section still obeys the blackbody spectrum (which was proved to be a good assumption for the source region , i.e. $q'' = f \sigma T^4$), and with plasma velocity of 12 km/s (exposure time per each single section is 1 μs) , this implies that the heat flux dropped by about 50% from its initial value during the exposure of the first 5 test sections. The approximately equal ablation of the subsequent 5 Lexan sections is indicative of equal heat flux along the last 5 sections of the sample indicating that the plasma temperature dropped by 16% from its initial value. An explanation for the drop may be due to the absorption of considerable fraction of the incoming energy to melt and vaporize the metallic copper surface and the vaporization of the high density graphite, with a variable f, while f is still constant for the subsequent Lexan sections. A final conclusion will depend upon more investigation and measurements for other specially-arranged samples, and modeling of the ablation process for surfaces with changeable specific enthalpy, which could be done in future.

MULTIPLE EXPOSURE OF MATERIAL SURFACES

Of concern in the design of EM launchers is the ability of exposed material surfaces to survive many shots without having to be replaced or cleaned. Experiments were conducted for the source insulator as well as the barrel side, for two test materials (Lexan and aluminum) at two different values of the input energy (1 and 1.7 kJ). The procedure for such type of experiments is to use a fresh sample and a fresh insulator sleeve and expose them to plasma at a preset input energy . Measuring the weight loss after the first shot then repeat the exposure 10 times with the weight loss to be measured between the shots . This procedure will be noted as the "ACCUMULATED" exposure. Another fresh sample and insulator sleeve were exposed without measuring the weight loss between the shots, this procedure will be noted as "MULTIPLE" exposure. Comparison between the accumulated and multiple exposures may help in obtaining a better view on the performance of the insulator and the barrel. Fig. 29 shows the behavior of the source insulator which indicates a linear behavior with increasing rate for accumulated shots, and less ablation for multiple shots which indicates the surface conditioning effect on the ablation process. For EM and ET applications, the maximum number of exposures which will produce a certain allowable increase in the bore diameter could be predicted. Fig. 30 shows comparison between aluminum barrels on accumulated and multiple exposures for two energy regimes, which indicates that the erosion, at all energies, is linearly increasing for accumulated shots and non-linearly for multiple shots with higher erosion rate. Fig. 31 shows the behavior of Lexan (as a test material inside the barrel), indicating that the multiple exposure is linear and the ablation rate is less than that of the accumulated exposure which has non-linear behavior at higher energies. This concludes that the metallic surfaces are not recommended for multiple exposure without cleaning between the shots, while multiple exposure is recommended for insulators at all energy values. Modeling of the accumulated and multiple

exposure will help in predicting the maximum number of useful shots (within a permissible tolerance) before either the insulator or the barrel of the launcher should be replaced.

MAGNETIC FIELD EFFECT

The magnetic field was applied at different field intensities (0 - 8.75 T) using splitted-Lexan samples at input energies of 4 and 5 kJ, in order to explore the Magnetic Vapor Shield (MVS) concept. Fig. 32 shows the effect of the magnetic field on the ablation depth along the sample axis at an input energy of 4 kJ. It is evident that lower values of the magnetic field (up to 5T) will enhance the rate of ablation, while higher values (greater than 5T) will reduce the ablation depth below that obtained with no magnetic field. The phenomena is not yet clearly understood, but it is conjectured that a threshold value for the magnetic field is required for the onset of the Magnetic Vapor Shielding effect. Fig. 33 shows the average ablation depth over the sample length at 4 and 5 kJ input energy, and it is apparent that, to be effective, the magnetic field at higher input energies should exceed 10T. The Optical spectra received end-on through a fiber optical cable connected to an optical multichannel analyzer showed a decrease in the relative intensity with the increase in applied magnetic field as shown in fig. 34, which may be indicative of the reduction of the ablated material. Further studies are necessary to explore the magnetic field effect.

CONCLUDING REMARKS

The project has been successful in designing, constructing and operating the proof-of-principle experiment SIRENS to simulate the exposure of material surfaces to high heat fluxes under EM and ET launchers conditions, with the following conclusions:

- Experimental verification of the vapor shield effect. Energy transmission factor through the vapor shield varies from 20% to 5% as the heat flux increases.

- Metals have strong axial erosion dependence, with average erosion depth of 15 - 45 μm/kJ for aluminum, and 5 - 10 μm/kJ for pure copper.

- Insulators have equal ablation along the axial direction, with average ablation depth of 10 - 14 μm/kJ for Lexan.

- Aluminum has higher erosion rate with increase of input energy, while Lexan and pure copper have approximately equal erosion rates which are considerably less than that of aluminum. High density graphite does not ablate at lower energies and slightly ablates at energies above 3 kJ, while molded dense electrographite ablates at higher rate, and both types of graphite are of considerable less ablation than the other materials. Lexan and graphite showed evidence of vapor shield effect rather than aluminum and copper, although the normalized erosion depth for aluminum and copper showed tendency towards less erosion rates at higher values of heat fluxes. The average ablation depth of high density graphite is 1 -2 μm/kJ, and for molded dense electrographite is 1 - 3 μm/kJ.

- Heat flux is approximately constant along the axial direction which indicates that the axial distribution of the plasma temperature does not change along the axis during the exposure time, with the average plasma velocity of 10-12 km/s. The metallic-insulator samples showed a reduction in the temperature of only 16% of its initial value.

- Multiple exposure of the material surfaces showed that the multiple exposure of the source insulator or barrel insulator decreases the ablation rate, while multiple exposure of metallic barrels increases the erosion rate. Conservative estimates showed that about 190 exposures (at 1 kJ input energy) cause an increase of 20% in the inner bore diameter.

- There is initial indications of a reduction in ablation with applied magnetic fields above 5 T, for insulator materials (Lexan).

REFERENCES

1. J. Gilligan and D. Hahn, "Magnetic Vapor Shielding Mechanism for Protection of High Heat Flux Components in High Field Tokamaks", Journal of Nuclear Materials, 147, 381-395 (1987).

2. J. Gilligan, O. Auciello, M. Bourham, O.Hankins, B. Wehring, D. Hahn, R. Mohanti and J. Stock, "Theoretical and Experimental Studies of the Vapor Shielding Mechanism for Surfaces Subject to High Heat Fluxes", Fusion Technology, 15, No.2, Part A, 522-527 (1989).

3. D. Keefer and R. Crawford, "Optical Diagnostics of Railgun Plasma Armatures", IEEE Trans. Magnetics, 25, No.1, 295-299 (1989).

4. O. Auciello, O. Hankins, B. Wehring, M. Bourham and J. Gilligan,"Proof-of-Principle Experiment for the Magnetic Vapor Shield Mechanism", Final Report, DOD Equipment Grant DAAL03-86-G-0157, Nov. 1987 .

5. A. Sestero, "Protection of Walls from Hard Disruptions in Large Tokamaks", Nuclear Fusion, 17, 115 (1977).

6. A. Hassanein, "Surface Melting and *Evaporation* During Disruption in Magnetic Fusion Reactors", Nuc. Eng. and Design/Fusion, 1, No.3 (1984).

7. D. Rosen, J. Mittledorf, G. Kothandarman, A. Piri, E. Pugh, "Coupling of Pulsed 0.35 um Laser Radiation to Aluminum Alloys", J. Appl. Phys., 53, 4, 3190 (1980).

8. M. Bourham, O. Hankins, O. Auciello, J. Stock, B. Wehring, R. Mohanti, J. Gilligan, "Vapor Shielding and Erosion of Surfaces Exposed to High Heat Load in an Electrothermal Accelerator", IEEE Trans. on Plasma Science, 17, No.3, 386-391 (1989).

9. J. Gilligan, M. Bourham, O. Auciello, O. Hankins, B. Wehring, "Fundamental Studies to Reduce High Heat Flux Erosion of Surfaces", (Invited) IEEE Conf. on Plasma Science, Seattle, WA, June (1988), IEEE Cat. No. 88CH2559-3.

10. J. Gilligan and R. Mohanti, "Time Dependent Numerical Simulation of Ablation Controlled Arcs", To be published in IEEE Trans. on Plasma Science, April 1990.

11. Graphite 6222 high density and Graphite 2020 molded dense electrographite, products of Stackpole Ultra Carbon Corporation, Bay City, MI 48708

PROJECT PUBLICATIONS

1. J. Gilligan, R. Mohanti, "Time Dependent Numerical Simulation of Ablation Controlled Arcs", accepted for publication, IEEE Trans. on Plasma Science (1990).

2. J. Gilligan, D. Hahn, R, Mohanti, "Vapor Shielding of Surfaces Subjected to High Heat Fluxes During a Plasma Disruption", Journal of Nucl. Mat. 162-164, 957-963 (1989).

3. J. Gilligan, O. Auciello, M. Bourham, O. Hankins, B. Wehring, D. Hahn, R. Mohanti, J. Stock, "Theoretical and Experimental Studies of the Vapor Shielding Mechanism for Surfaces Subjected to High Heat Fluxes", Fusion Technology 15, No. 2, Part 2A, 522-527 (1989).

4. M. Bourham, O. Hankins, O. Auciello, J. Stock, B. Wehring, R. Mohanti, J. Gilligan, "Vapor Shielding and Erosion of Surfaces Exposed to High Heat Load in an Electrothermal Accelerator", IEEE Trans. on Plasma Science 17, No. 3, 386-391 (1989).

5. O. Hankins, J. gilligan, B. Wehring, M. Bourham, O. Auciello, "Multiple-Use Plasma Laboratory for Graduate Fusion Education", Trans. Am. Nuc. Soc. 59, 106-107 (1989).

6. J. Gilligan, D. Hahn, R. Mohanti, "Modelling of the Vapor Shield Mechanism During High Heat Flux Ablation of Surfaces", IEEE Plasma Science Conf. Proc., IEEE Cat. No. 89CH2760-7, 40 (1989).

7. O. Hankins, M. Bourham, O. Auciello, J. Stock, J. Gilligan, B. Wehring, "Parametric Studies of High Heat Flux Induced Erosion of Surfaces in an Electrothermal Accelerator", IEEE Plasma Science Conf.Proc., IEEE Cat. No. 89CH2760-7, 60 (1989).

8. J. Gilligan, M. Bourham, O. Hankins, J. Stock, S. Tallavarjula, O. Auciello, "Erosion of Surfaces Exposed to Plasmas in an Electrothermal Accelerator", Bul. Am. Phys. Soc., 34, No. 9, 2030 (1989).

9. J. Gilligan, M. Bourham, O. Auciello, O. Hankins, B. Wehring, "Fundamental Studies to Reduce High Heat Flux Erosion of Surfaces", (Invited) IEEE Conf. on Plasma Science, Seattle, WA, June (1989), IEEE Cat. No. 88CH2559-3 .

10. J. Gilligan and D. Hahn, "The Magnetic Vapor Shielding Mechanism for Protection of High Heat Flux Components in High Field Tokamaks", Journal of Nuclear Materials 145-147, 391-395 (1987).

11. J. Gilligan, D, Hahn, "The MVS Mechanism for Protection of High Heat Flux Components in CIT Devices", Trans. Am. Nuc. Soc., 54, 117 (1987).

12. J. Gilligan, D. Hahn, "Energy Transport Through a Plasma Boundary Layer at a High Heat Flux Surface", Bull. Am. Phys. Soc. 32, No. 9, 1944 (1987).

13. O. Hankins, O. Auciello, M. Bourham, J. Gilligan, B. Wehring, "Control of Surfac Melting and Ablation via the MVS Mechanism", Proceedings of the 40th Annual Gaseous Electronics Conference, 181 (1987).

14. J. Gilligan, D. Hahn, "The Magnetic Vapor Shielding Mechanism for Protection of Components Subjected to High Heat Flux", Proc. IEEE Int. Conf. on Plasma Science, Arlington, VA, June (1987), IEEE Cat. No. 87CH2451-3 .

15. O. Auciello, O. Hankins, B. Wehring, M. Bourham, J. Gilligan, "Proof-of-Principle Experiment for the Magnetic Vapor Shield Mechanism", Final Report, DOD Equipment Grant DAAL03-86-G-0157, Nov. 1987 .

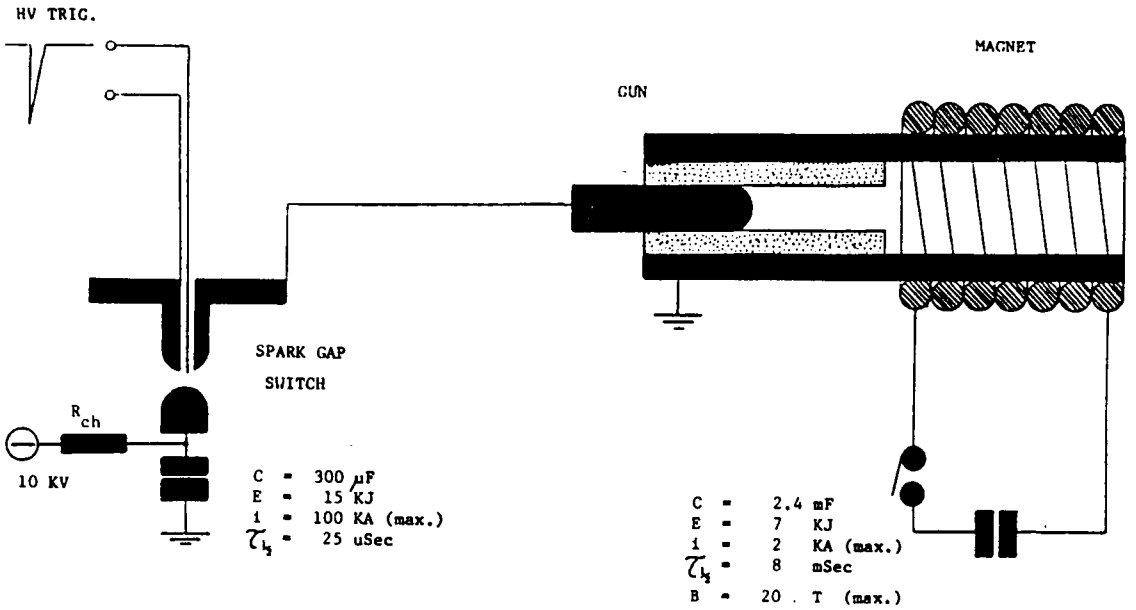

Fig. 1 Schematic drawing of SIRENS showing the source and test sections and the spark-gap switch, magnet and power supplies.

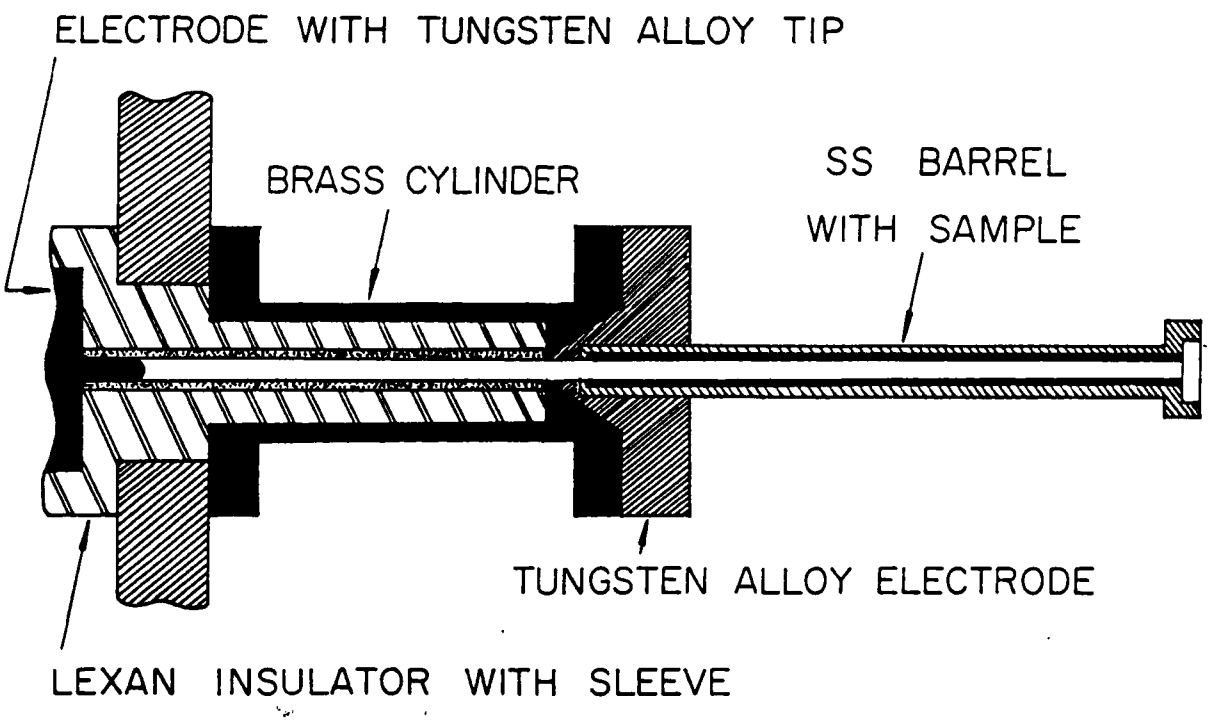

Fig. 2 Detailed drawing of the source and the barrel.

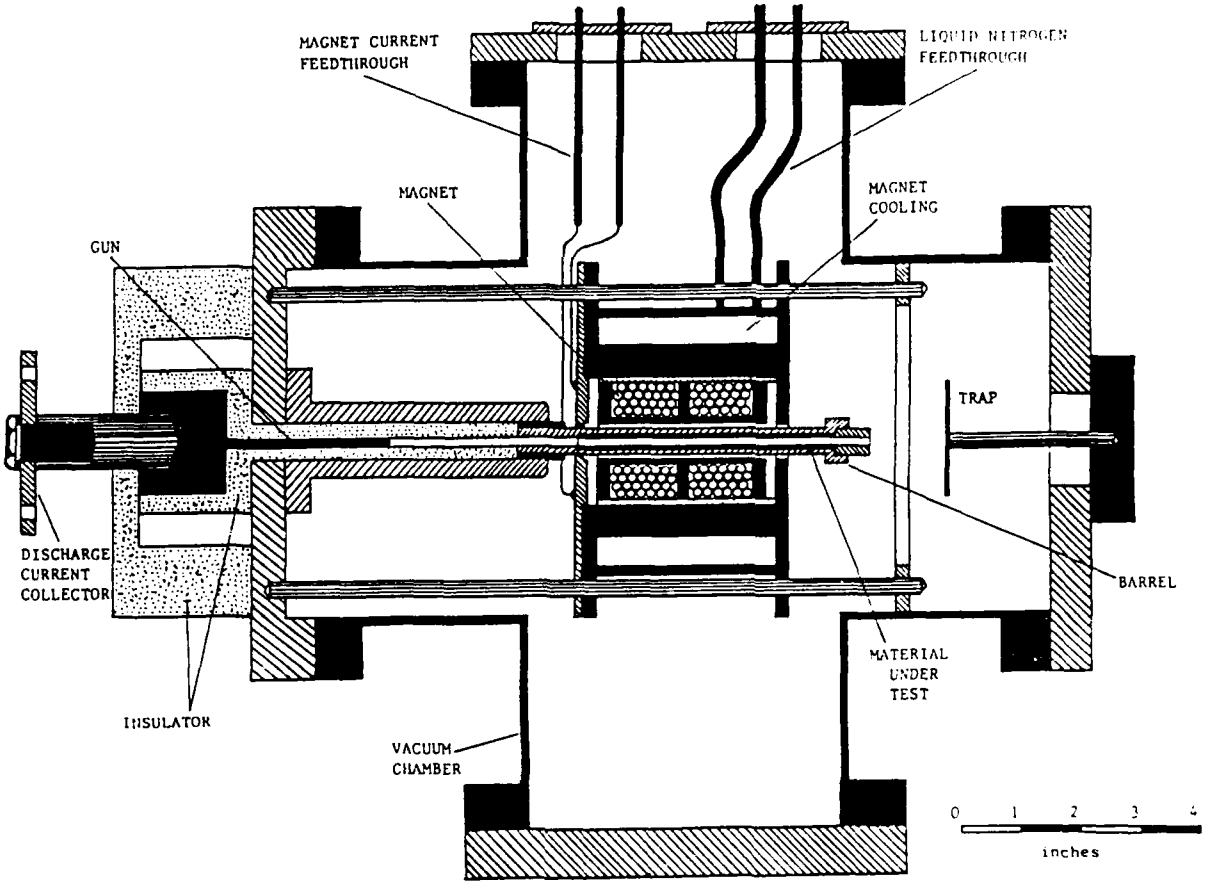

PLASMA GUN ASSEMBLY

PT. NO.	PART NAME	MATERIAL	NO. OF PCS.
1	EXPANSION COPPER ELECTRODE	COPPER	1
2	BARREL SUPPORT TO THE GUN SIDE	ST. ST.	1
3	BARREL	ST. ST.	1
4	BARREL END STUB	ST. ST.	1
5	MAGNET SPOOL	PLEXYGLAS	1
6	BARREL/SPOOL HOLDER	ST. ST.	1
7	SIDE COMPACT CLOSING	ST. ST.	1
8	MAGNET COOLING ASSEMBLY	ST. ST.	1
9	SUPPORTING SIDE FLANGE	ST. ST.	1
10	SUPPORTING COLLAR	ST. ST.	1
11	MAGNET ASSEMBLY SUPPORTING BOLTS	ST. ST.	4
12	SUPPORTING SLEEVES	ST. ST.	4
13	INSULATING CYLINDER	PLEXYGLAS	1
14	GUN MAIN ELECTRODE INSULATOR	PLEXYGLAS	1
15	GUN ELECTRODE	COPPER	1
16	GUN ELECTRODES' INSULATOR	PLEXYGLAS	1

Fig. 3 Assembly cross-section elevation of SIRENS and parts list.

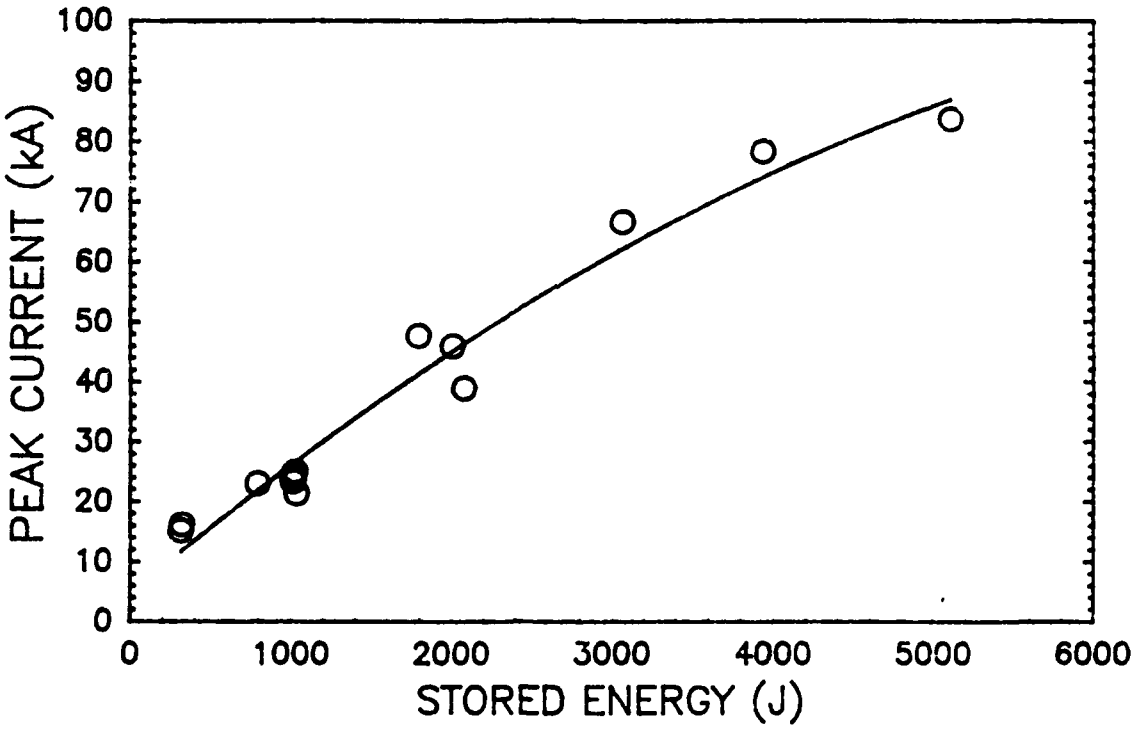

Fig. 4 Peak discharge current for different values of input energy .

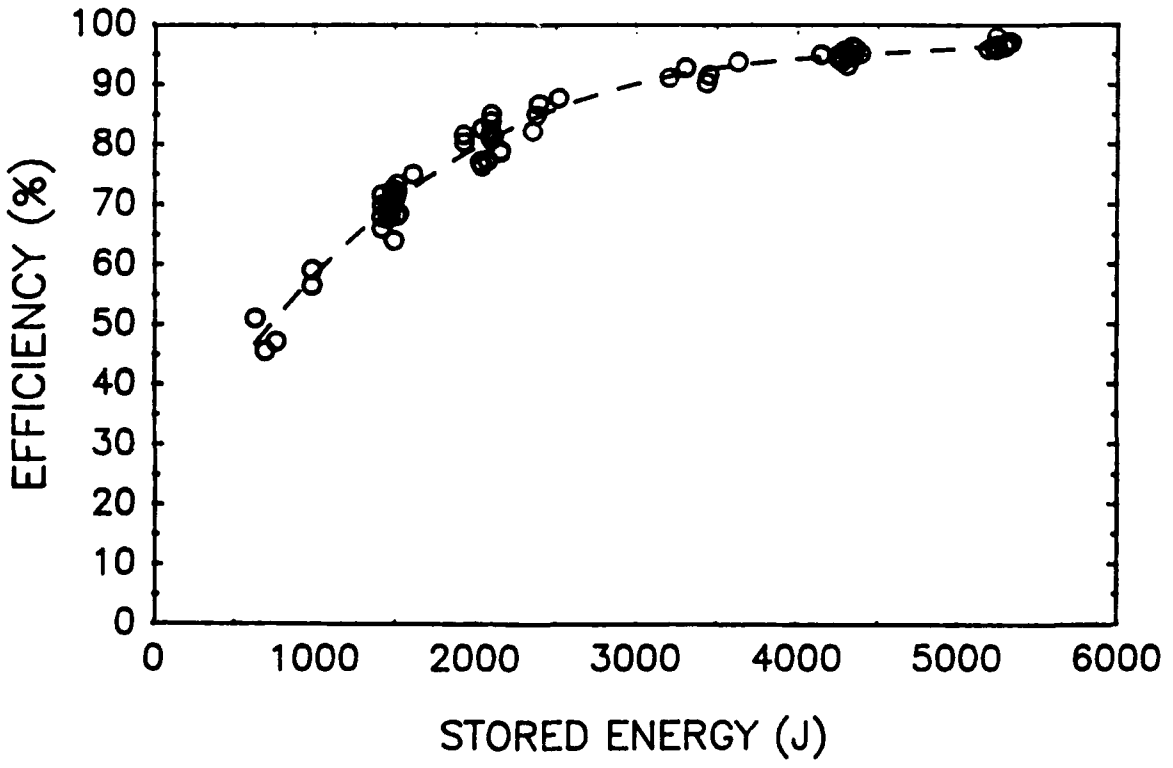

Fig. 5 SIRENS efficiency VS the stored energy of the capacitor.

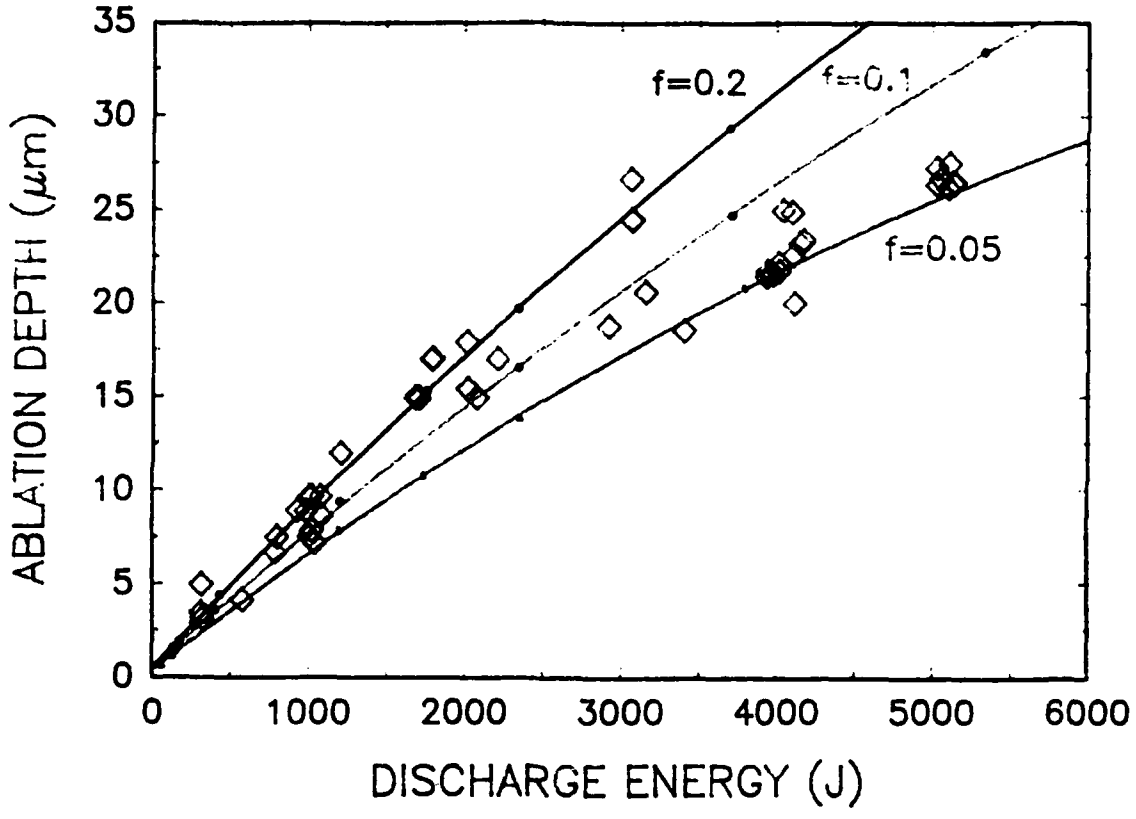

Fig. 6 Ablation depth of the source insulator (Lexan), Solid lines represent the predicted ablation depth as calculated theoretically by the ZEUS Code for different values of "f", and the experimental values show that f varies between 20% to 5% .

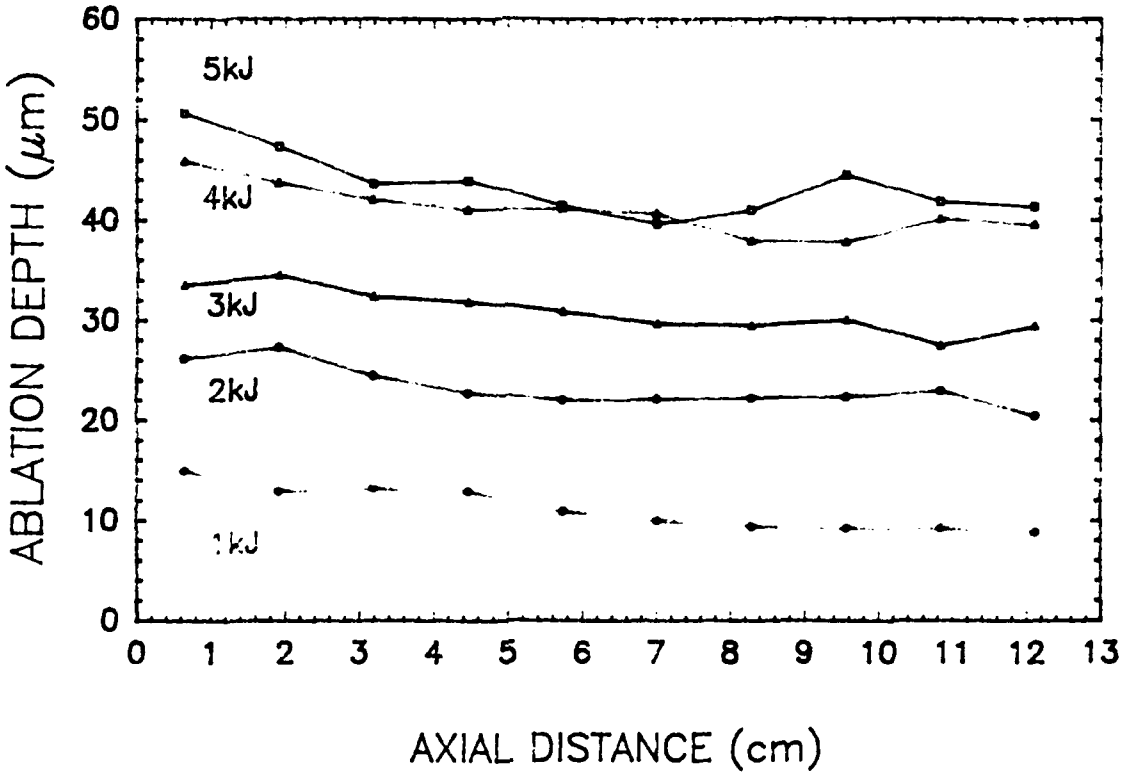

Fig. 7 Axial dependence of Lexan at different values of the input energy.

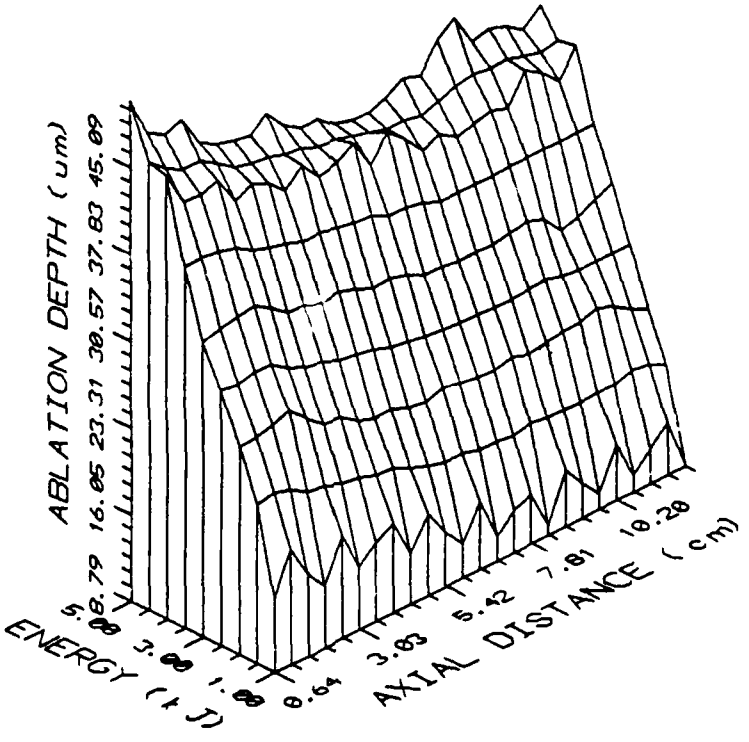

Fig. 8 3-D plotting of Lexan ablation along the axial direction at different values of the energy input to plasma.

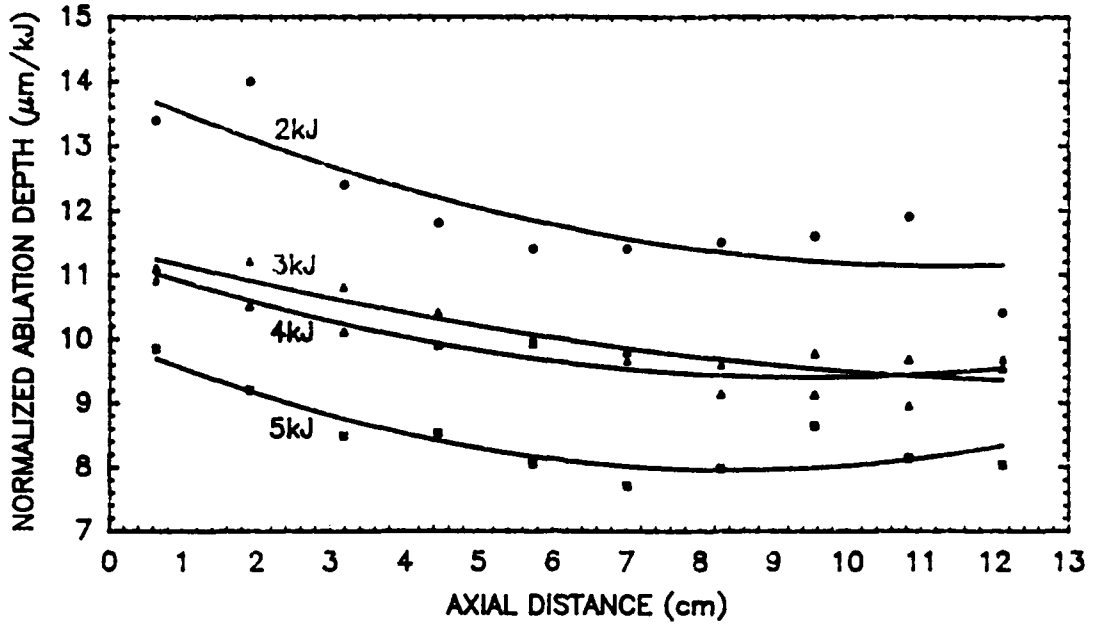

Fig. 9 Normalized ablation depth of Lexan at different values of energy input to plasma.

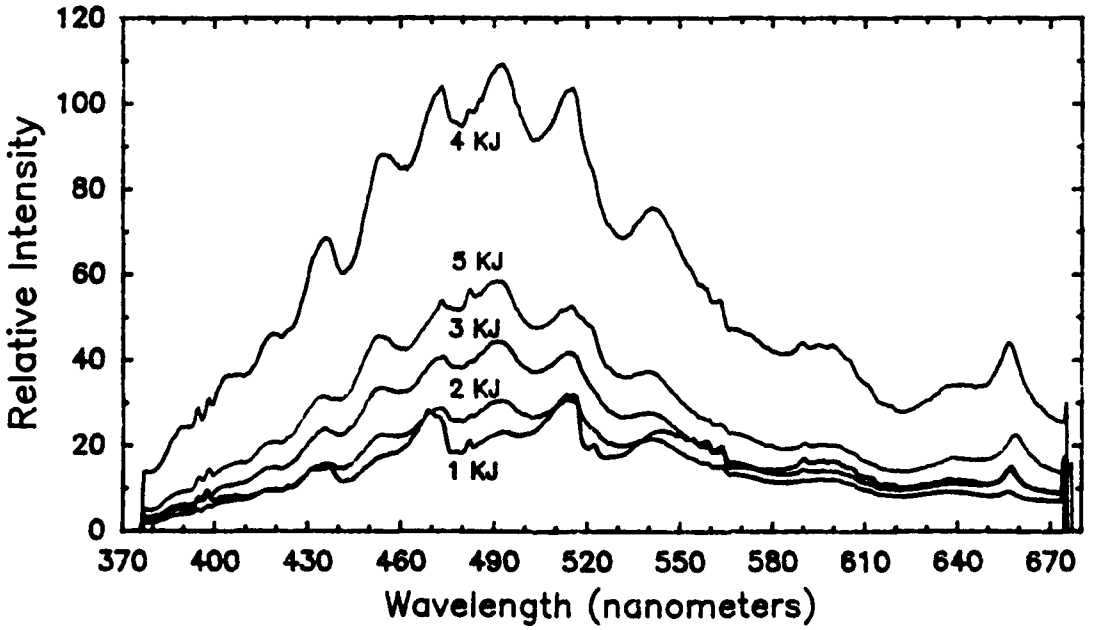

Fig. 10 Optical spectra received end-on during Lexan exposure to plasma.

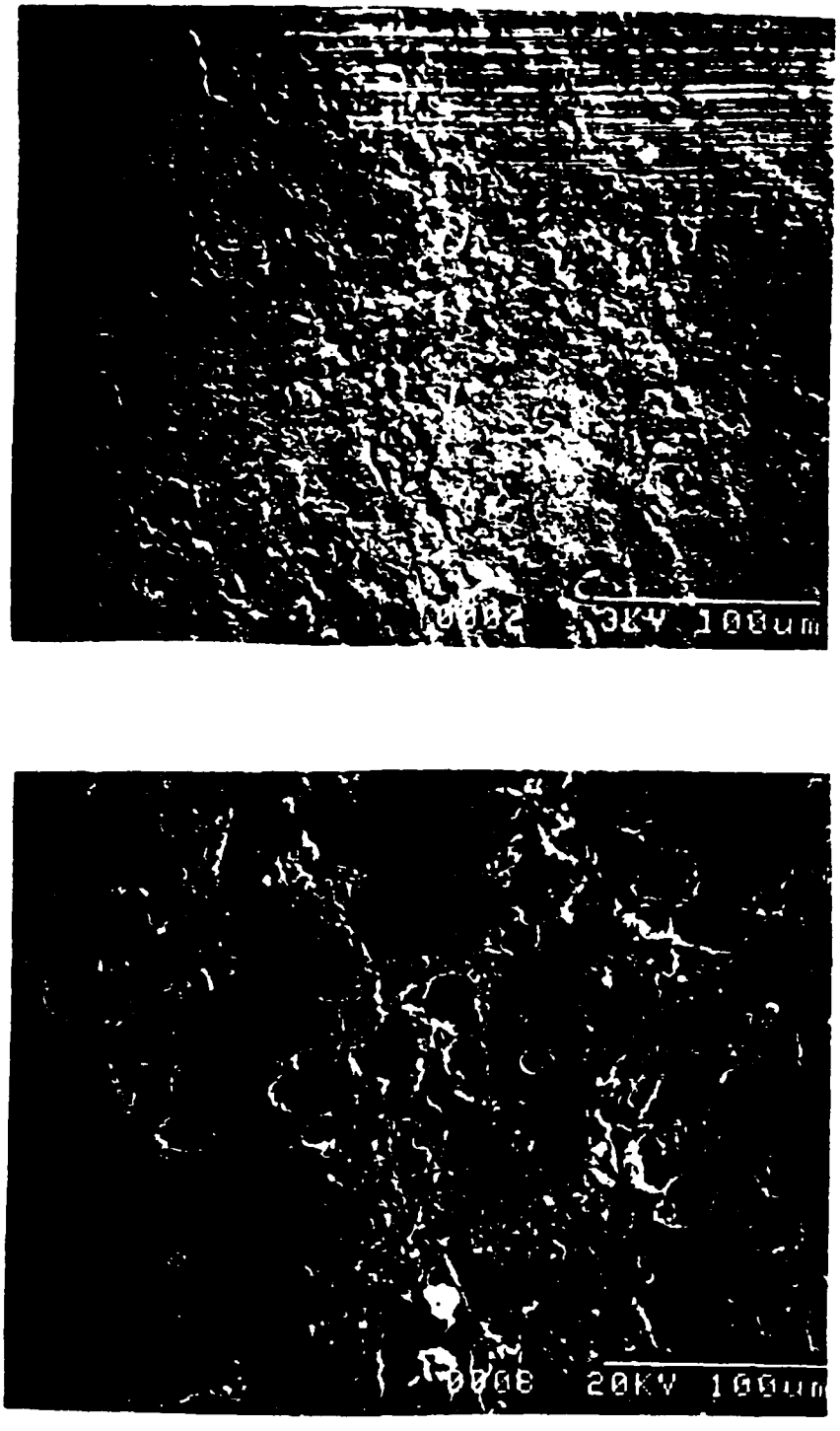

Fig. 11 SEM photographs of Lexan surface exposed to 5 kJ plasma.

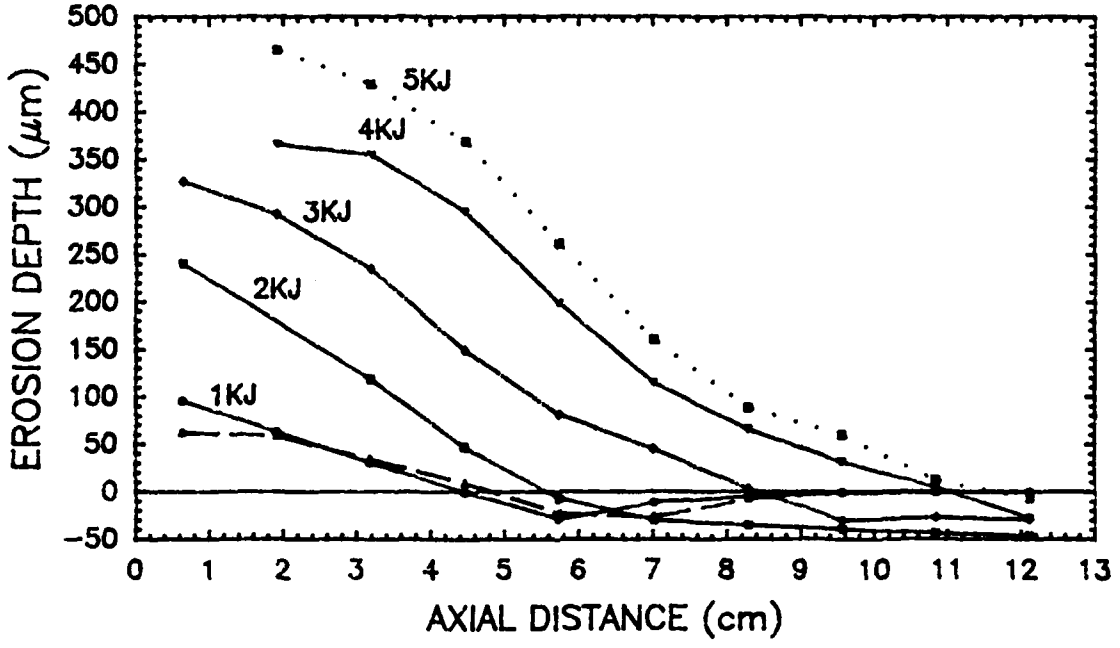

Fig. 12 Erosion depth of Aluminum along the axis at energies between 1 and 5 kJ .

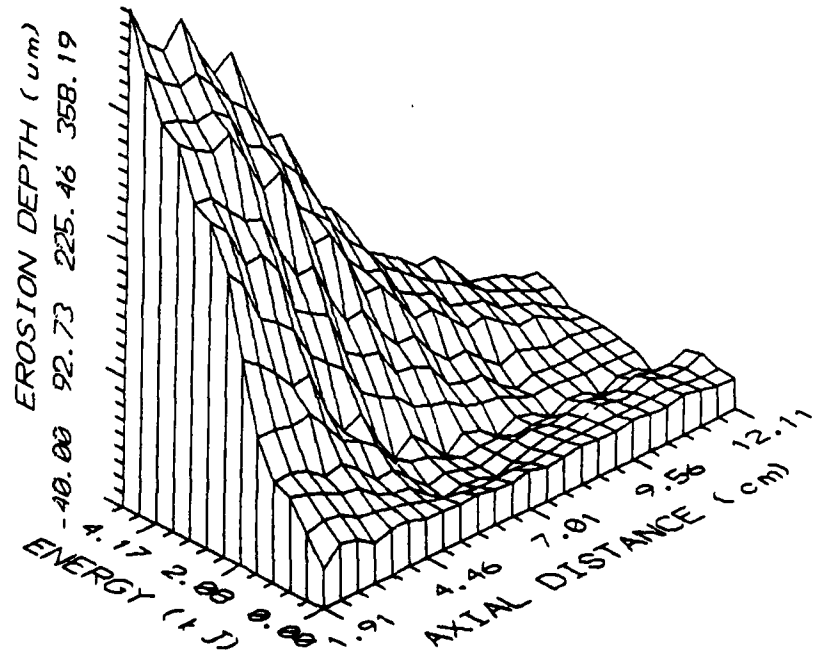

Fig. 13 3-D plotting of Aluminum erosion depth along the axial direction at different values of energy input to plasma.

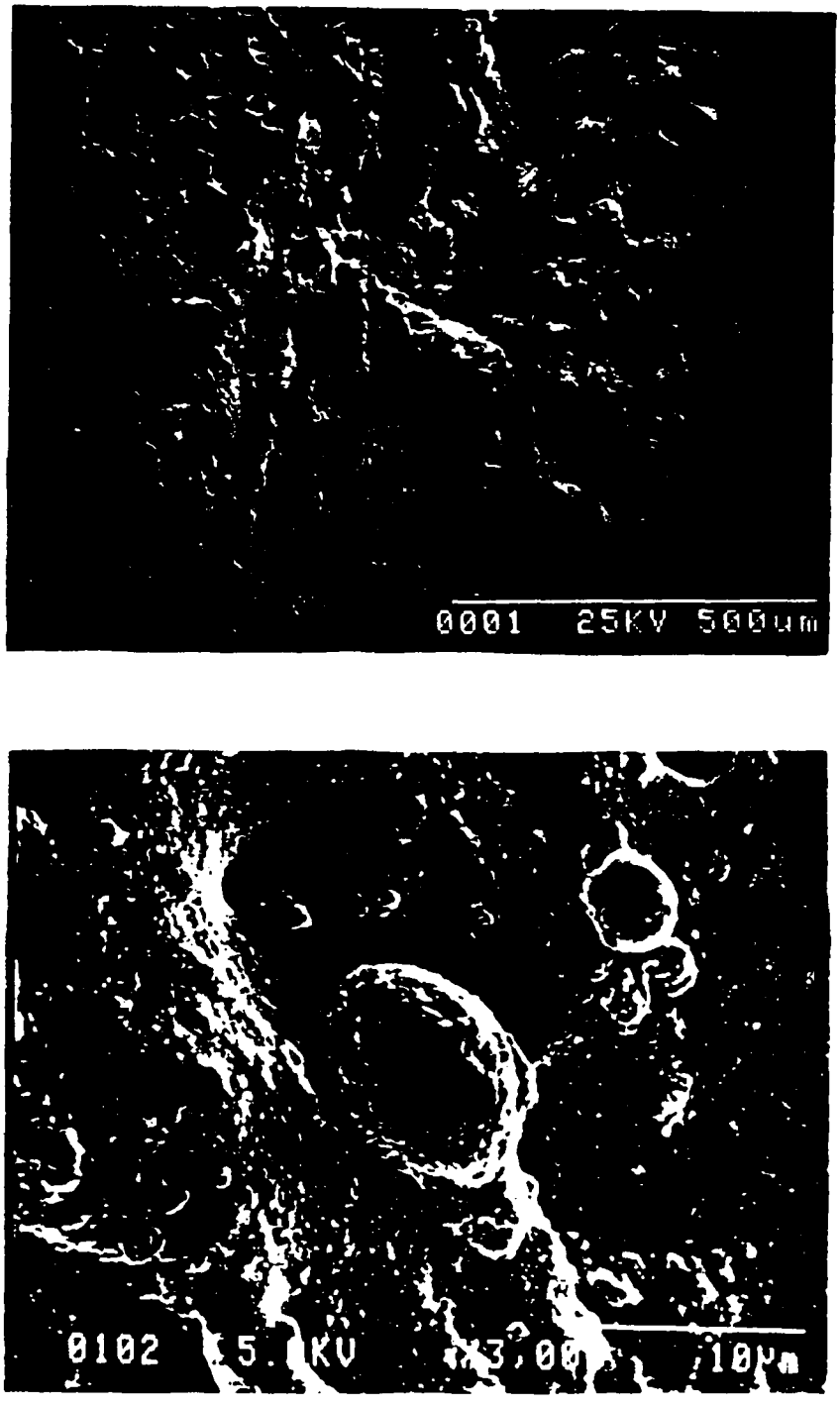

Fig. 14 SEM photographs of the exposed aluminum at 3 kJ input energy. Upper photo shows the features of the surface and the lower one (at higher magnification) shows features of resolidified material.

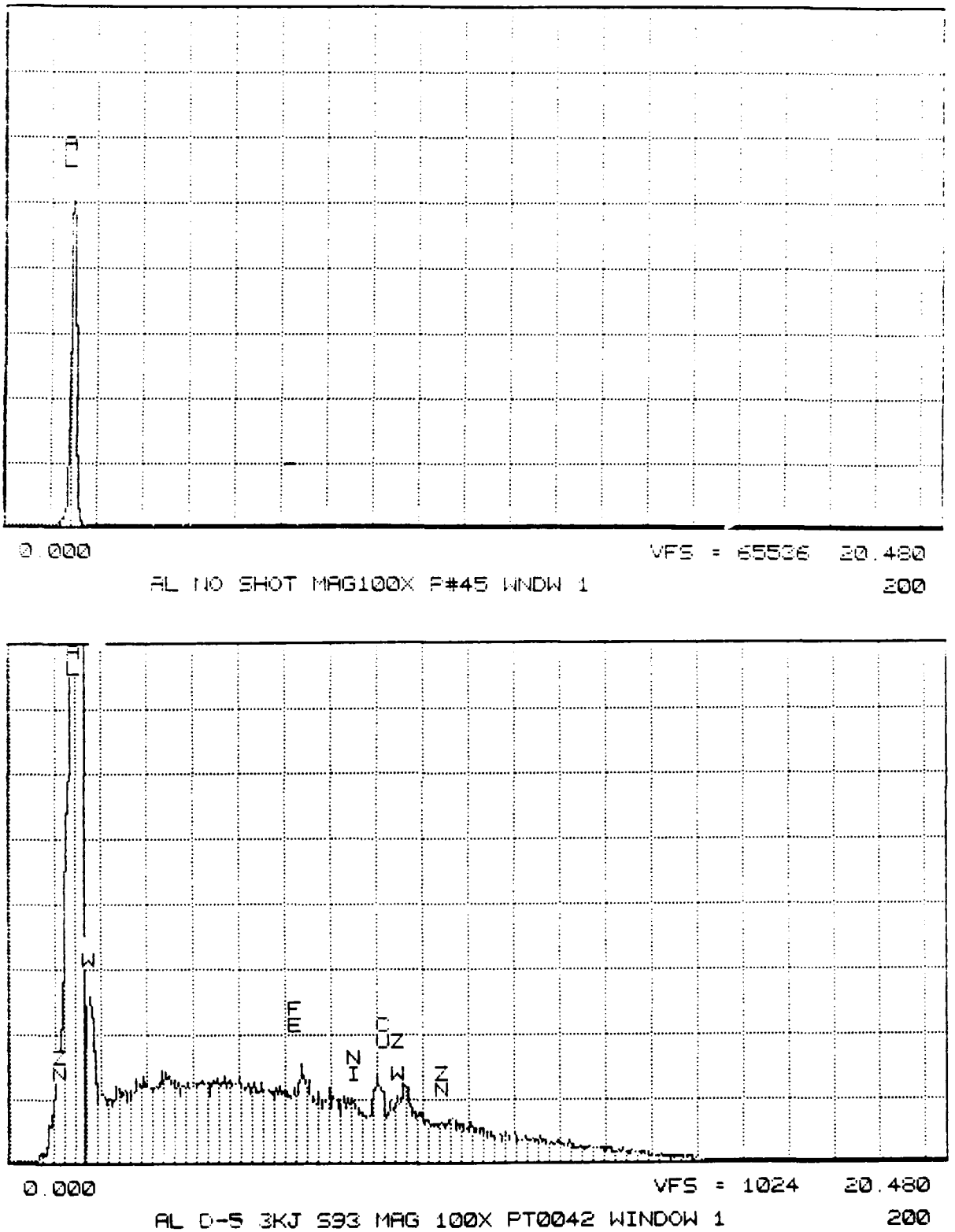

Fig. 15 EDXA analysis of non-exposed (upper) and exposed (lowe) aluminum at 3 kJ input energy. The non-exposed sample shows the aluminum peak while the exposed sample indicates peaks of aluminum, copper, nickel, zink, iron and tundsten.

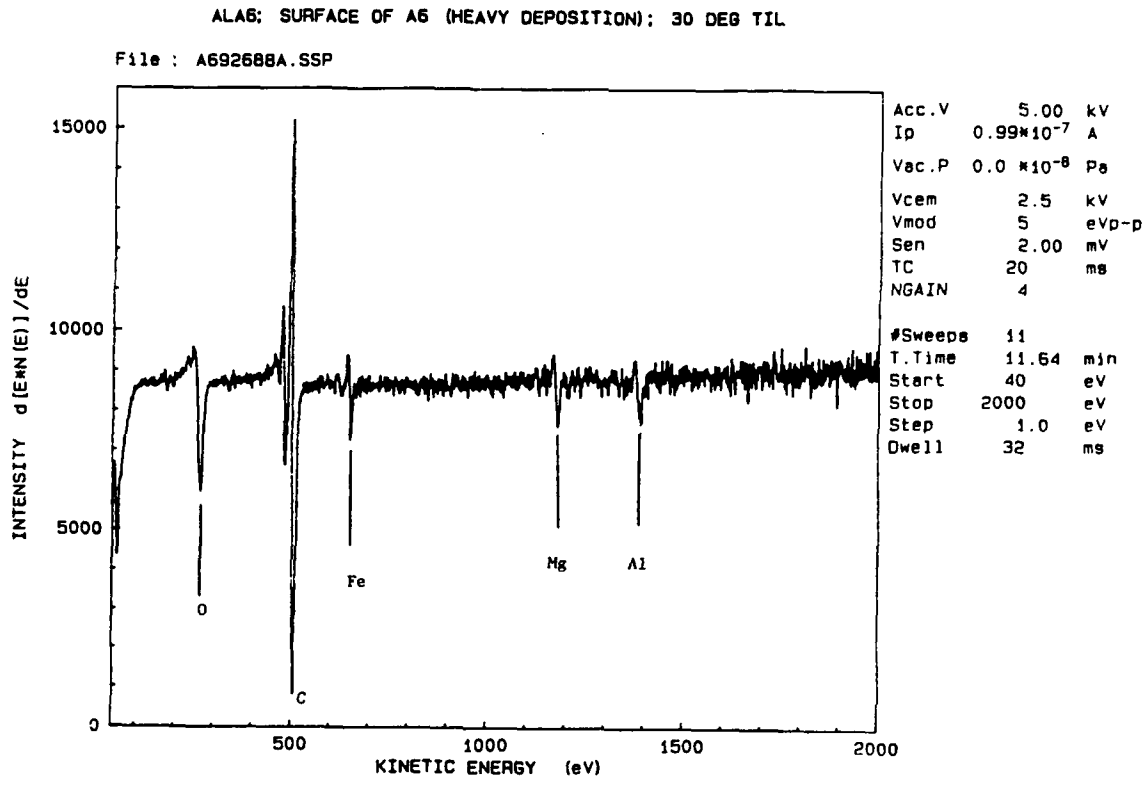

Fig. 16 Auger microprobe analysis of aluminum exposed to 3 kJ plasma.

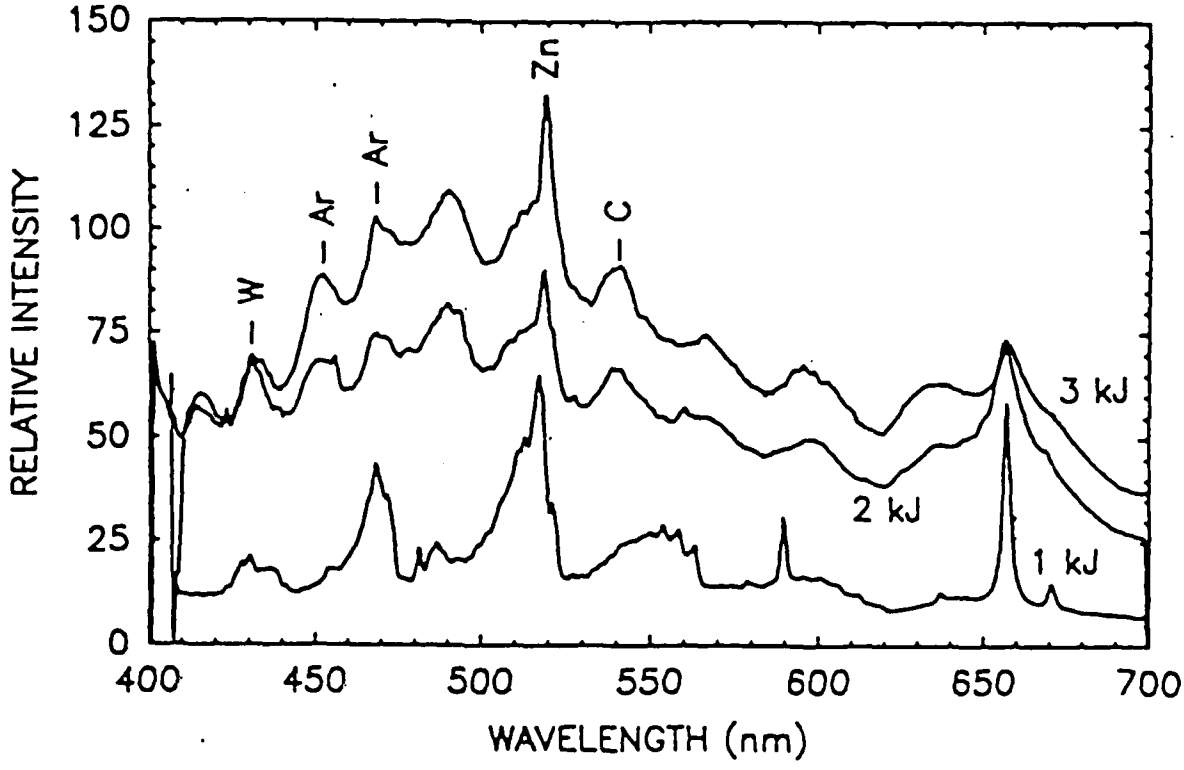

Fig. 17 Optical spectra received end-on showing carbon, argon, zink and tungsten lines.

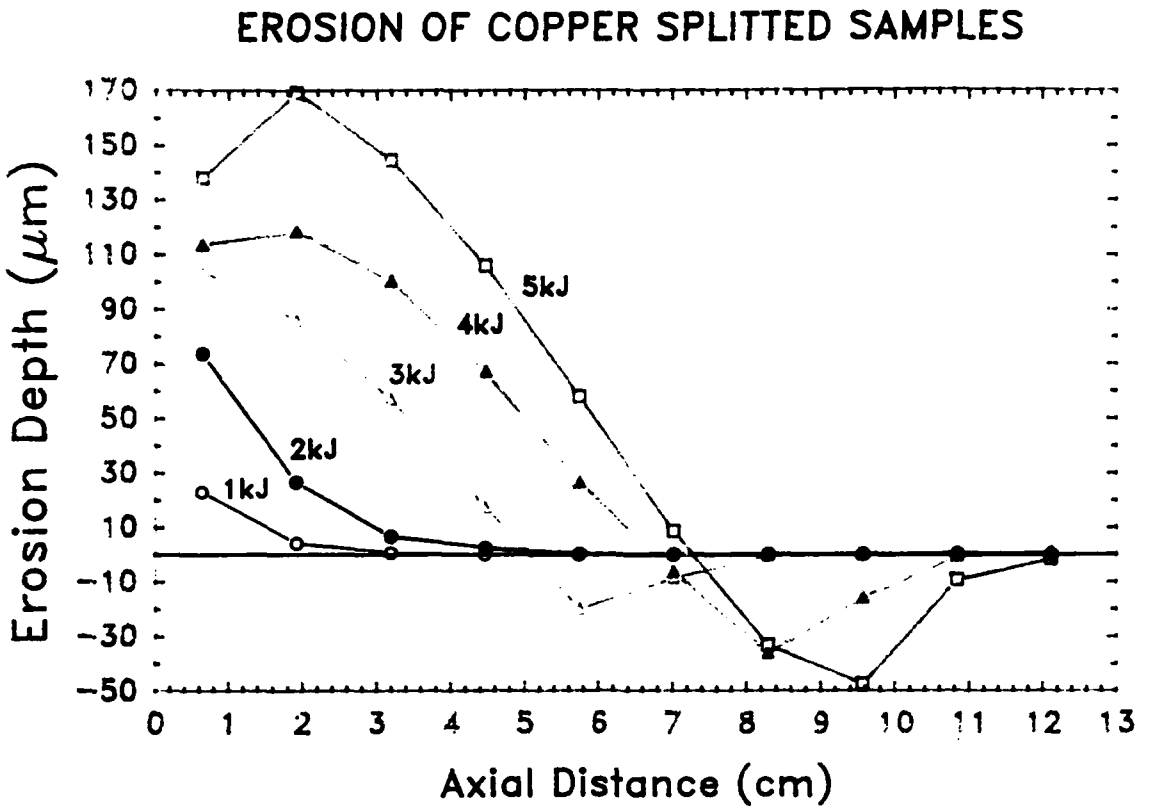

Fig. 18 Erosion depth of copper along the axial direction at energies between 1 and 5 kJ .

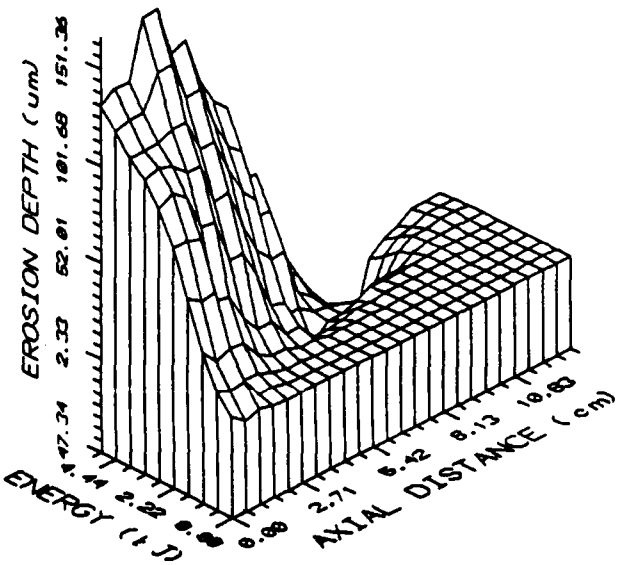

Fig. 19 3-D plotting of the exposed copper at energies between 1 and 3 kJ along the axis of the barrel.

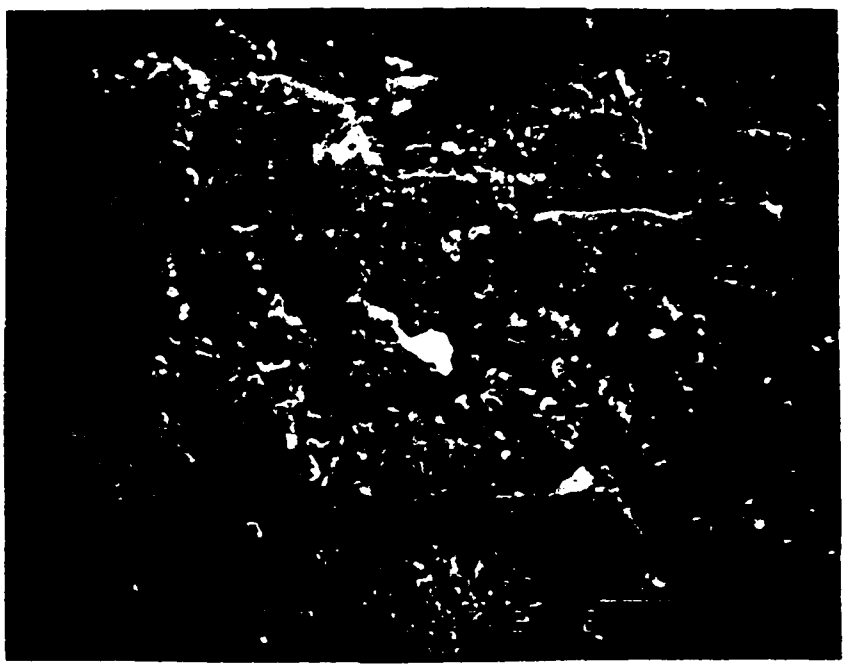

Fig. 20 SEM photographs of the exposed copper surface at 3 kJ input energy. Melting and resolidification is clear from the photographs.

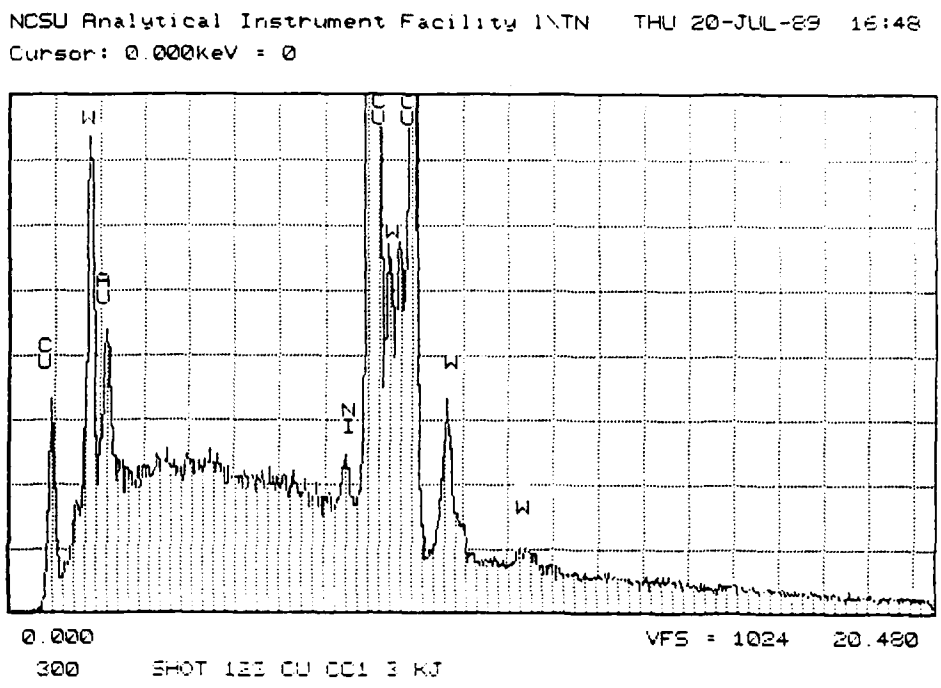

Fig. 21 EDXA analysis of exposed copper at 3 kJ input energy. Nickel and tungsten peaks are due to the erosion of the source electrode. The gold peak is due to gold-coating of the sample prior to EDXA analysis.

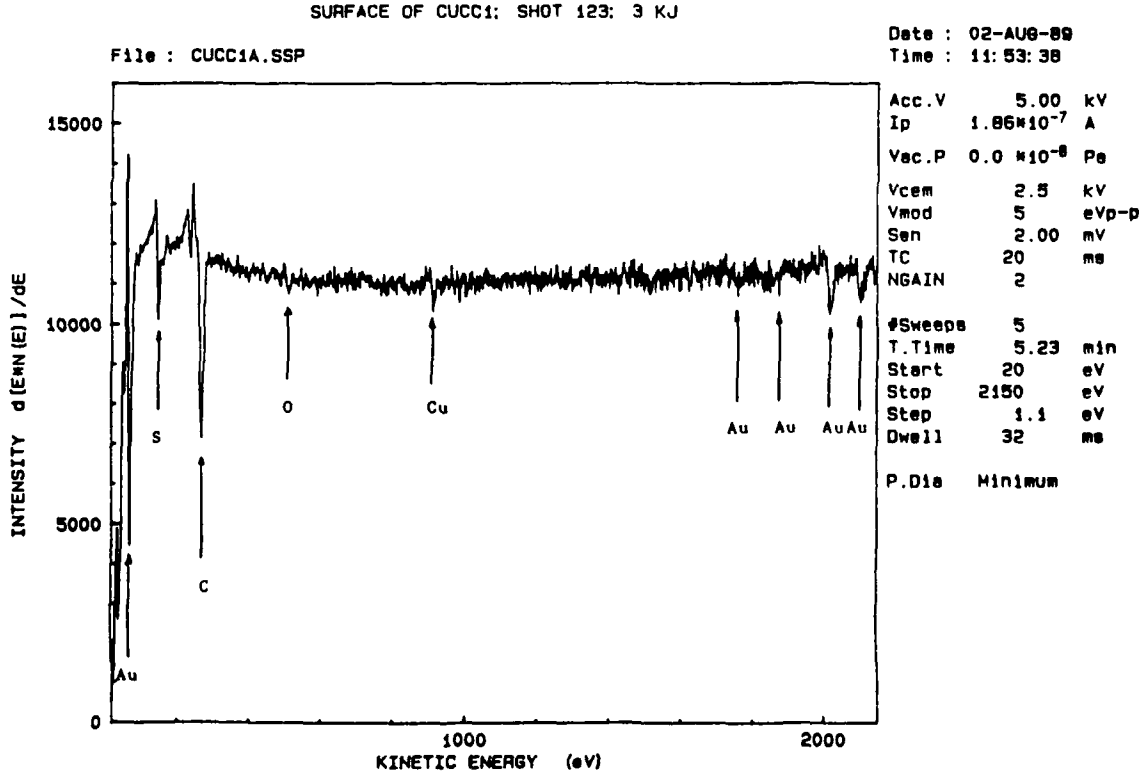

Fig. 22 Auger microprobe analysis of the exposed copper at 3 kJ input energy. Gold peaks are due to gold-coating prior to Auger analysis.

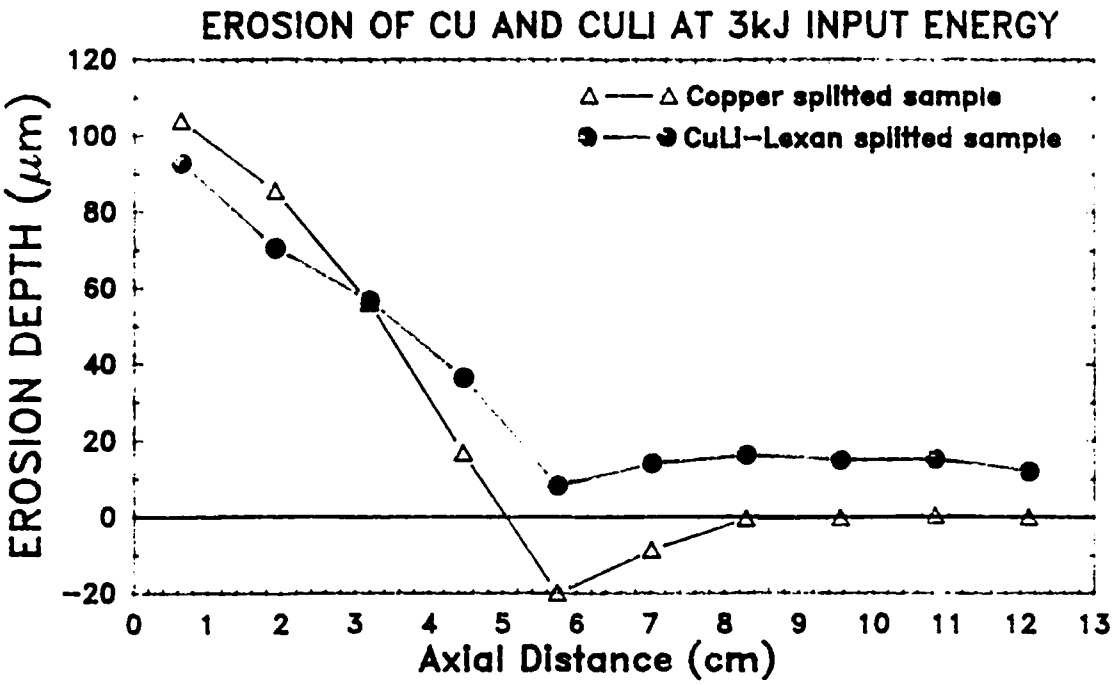

Fig. 23 Comparison between copper and copper-lithium erosion at 3 kJ input energy. The last 5 sections of the Cu-Li sample are from Lexan.

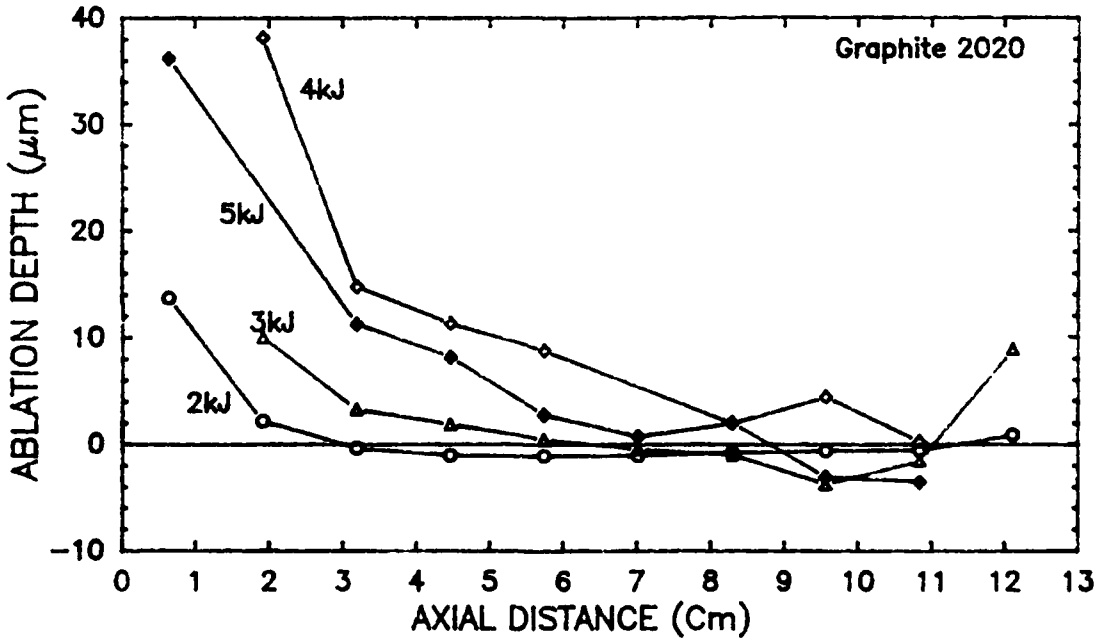

Fig. 24 Ablation depth of the molded dense electrographite (grade 2020) at energy inputs between 2 and 5 kJ.

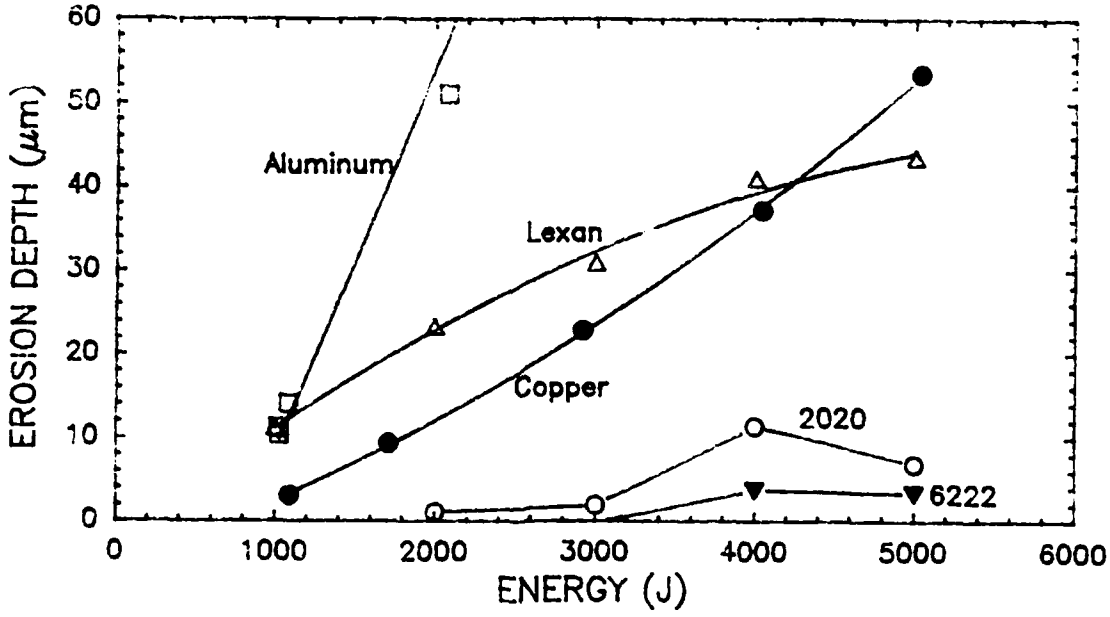

Fig. 25 Erosion depth of different materials at input energies between 1 and 5 kJ, averaged over the barrel length over the total time of exposure.

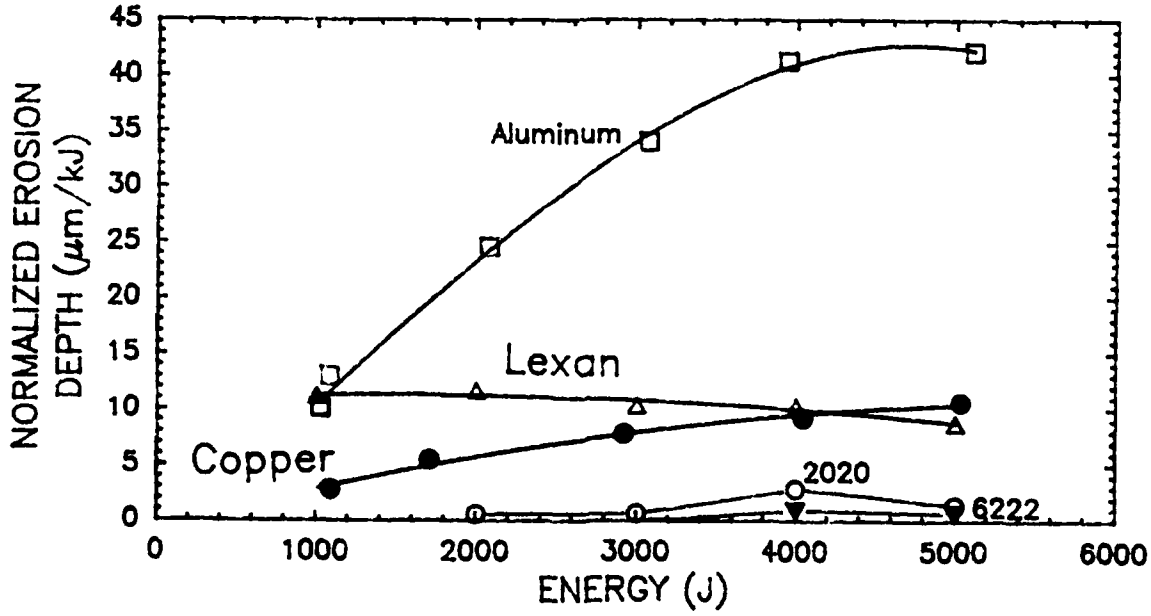

Fig. 26 Normalized erosion depth of different materials for input energies between 1 and 5 kJ .

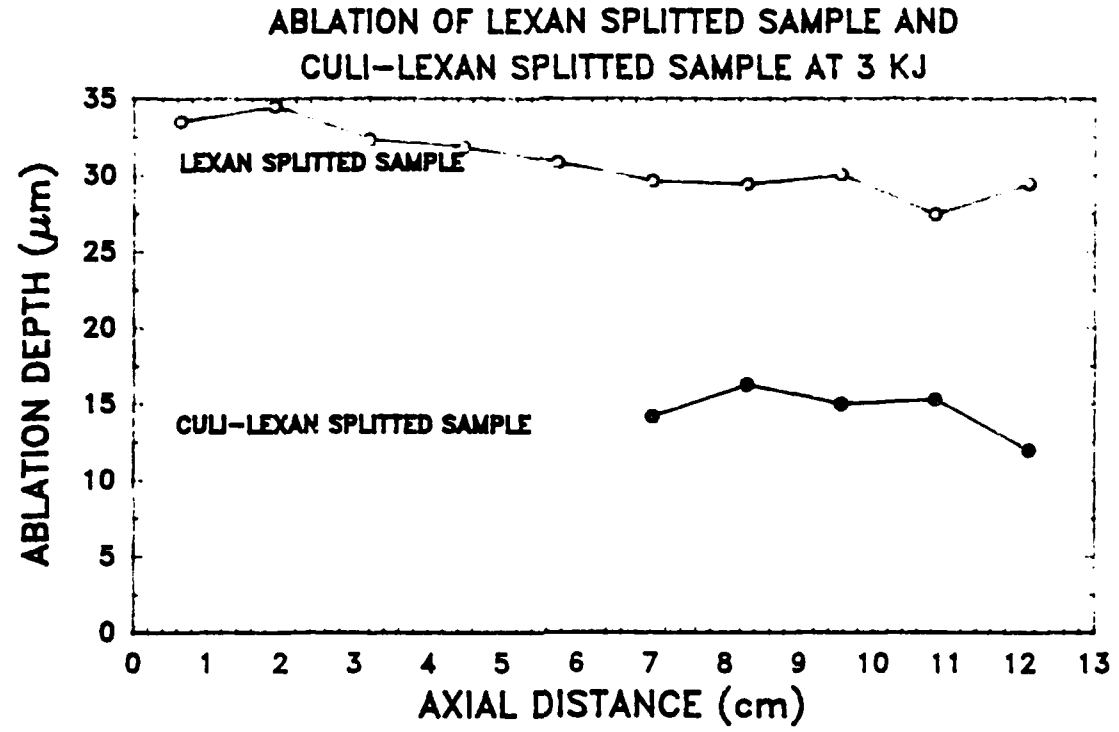

Fig. 27 Comparison between Lexan and CuLi-lexan samples at 3 kJ .

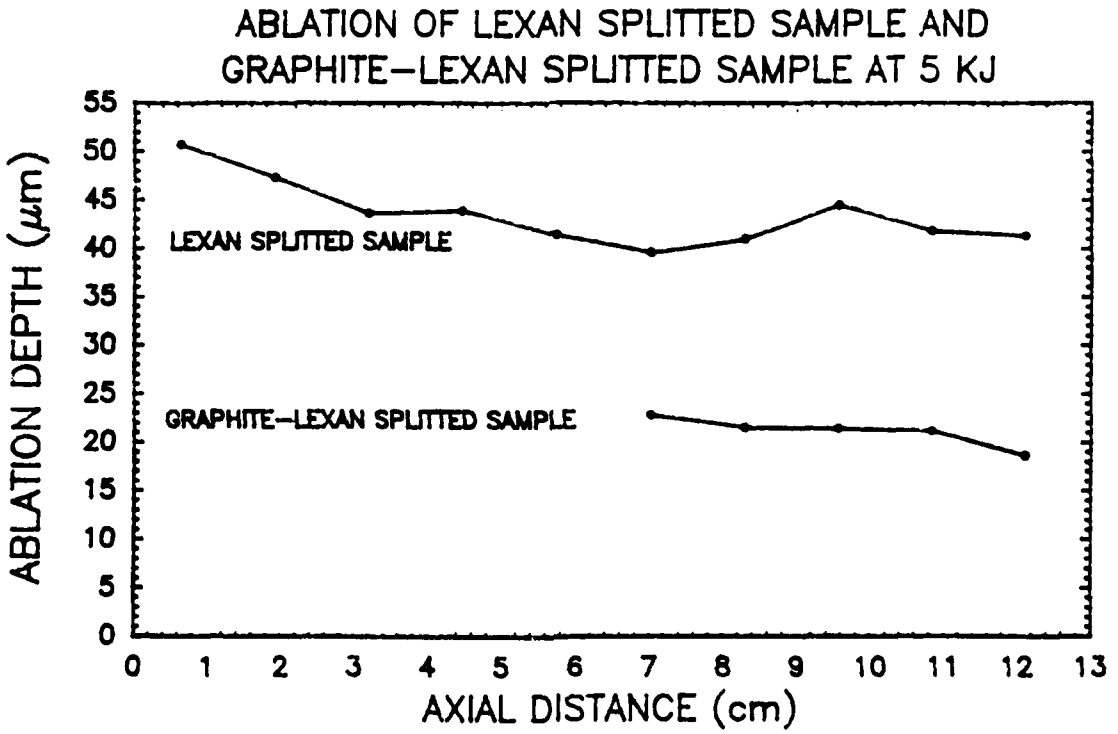

Fig. 28 Comparison between Lexan and Graphite-lexan at 5 kJ .

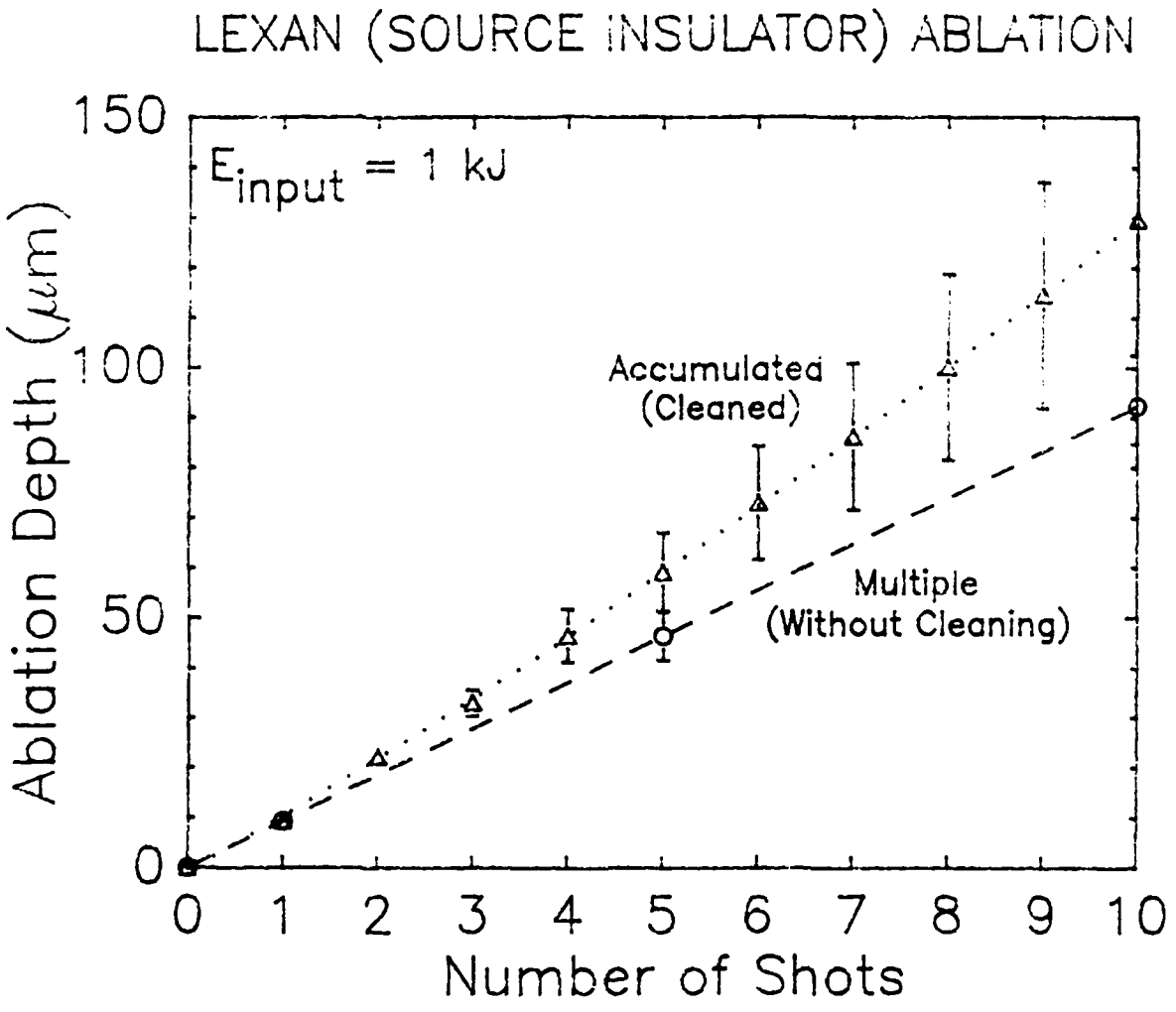

Fig. 29 Ablation of source insulator (Lexan) for accumulated and multiple regimes.

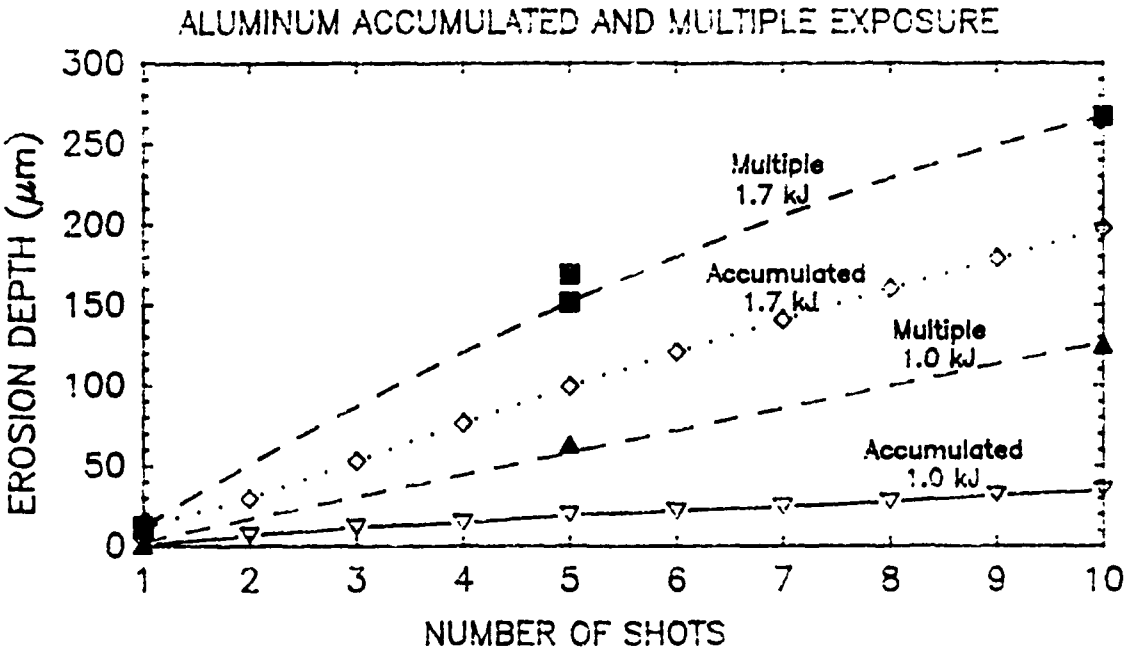

Fig. 30 Comparison between the aliminum erosion for multiple and accumulated regimes at two different values of energy input to plasma.

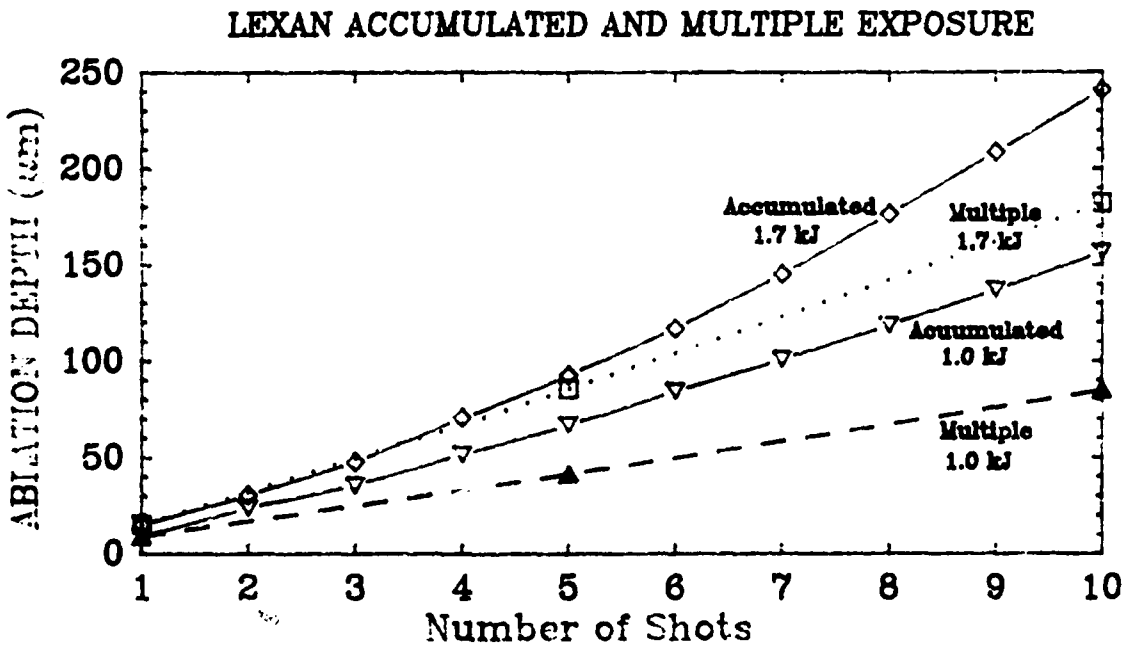

Fig. 31 Comparison between Lexan ablation for multiple and accumulated regimes at two different values of energy input to plasma.

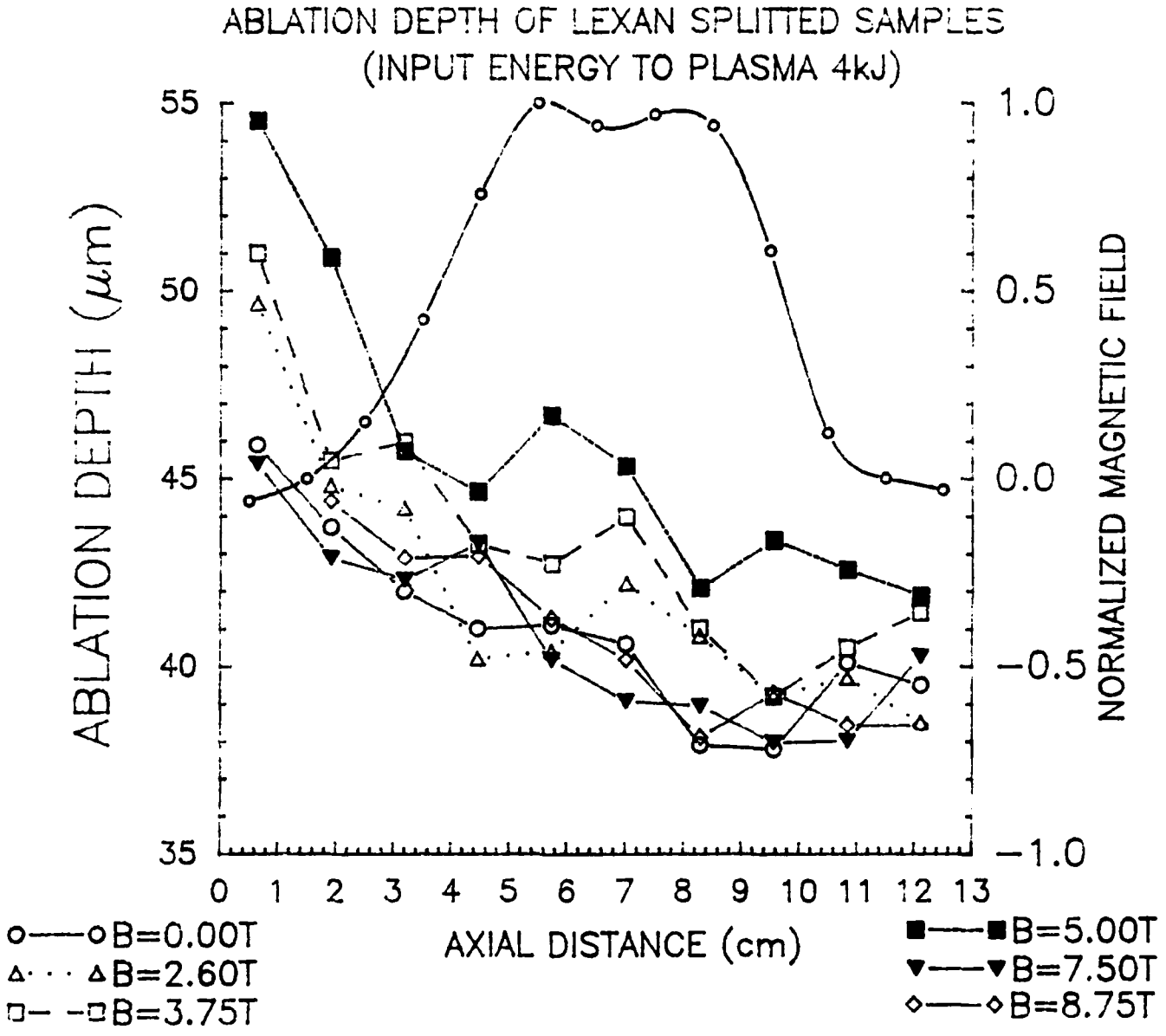

Fig. 32 Effect of the applied magnetic field on the ablation depth of Lexan along the barrel axis. Magnetic field varies from zero to 8.75 Tesla. The normalized magnetic field scale indicates the field distribution along the axial direction.

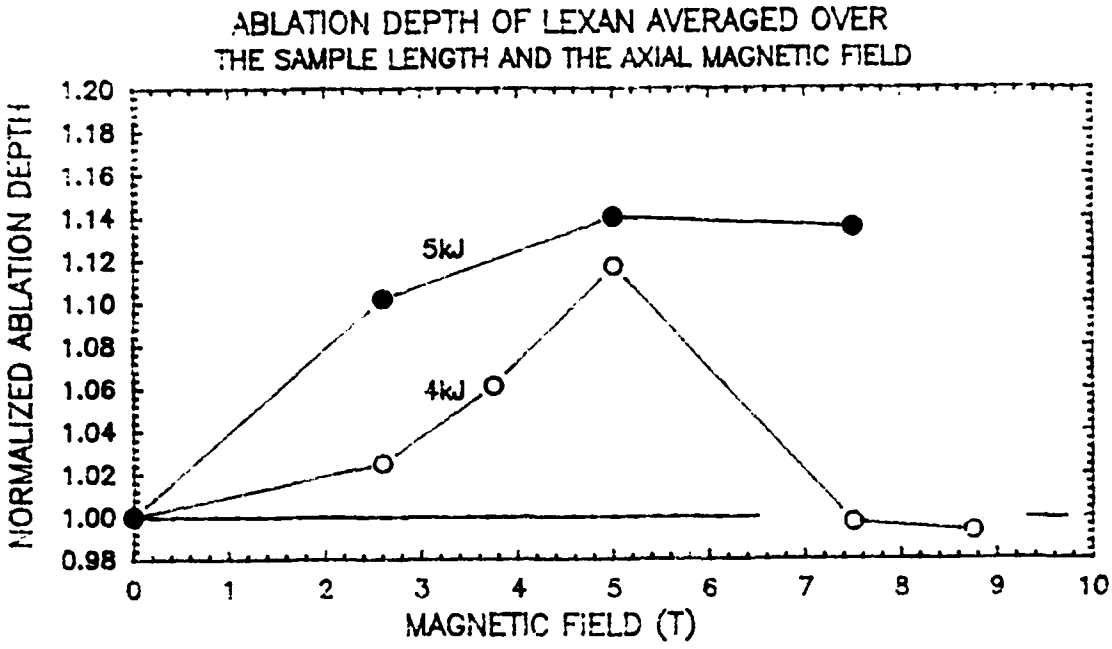

Fig. 33 Averaged ablation depth of Lexan at different values of the applied axial magnetic field. The values are normalized with respect to the ablation depth without magnetic field.

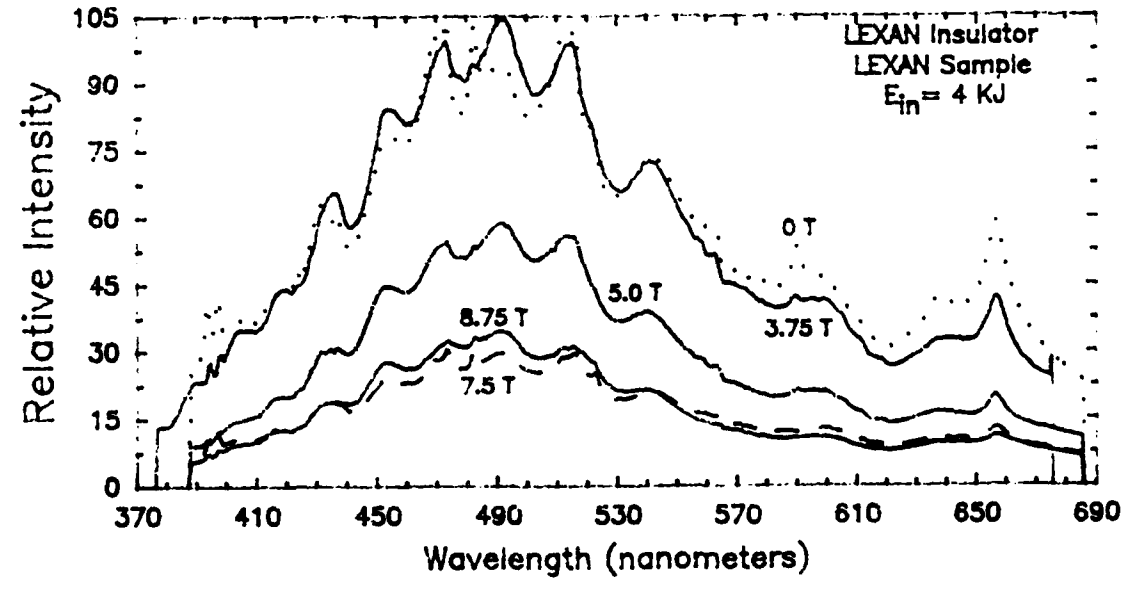

Fig. 34 Optical spectra received end-on during the magnetic field shots, at an input energy of 4 kJ .